Organometallic Complexes for Nonlinear Optics. 22.[1] Quadratic and Cubic Hyperpolarizabilities of *trans*-Bis(bidentate phosphine)ruthenium *σ*-Arylvinylidene and *σ*-Arylalkynyl Complexes

Stephanie K. Hurst,[†] Marie P. Cifuentes,[†] Joseph P. L. Morrall,[†] Nigel T. Lucas,[†] Ian R. Whittall,[†] Mark G. Humphrey,*[,†] Inge Asselberghs,[‡] André Persoons,[‡] Marek Samoc,[§] Barry Luther-Davies,[§] and Anthony C. Willis[∥]

Department of Chemistry, Australian National University, Canberra, Australian Capital Territory 0200, Australia, Centre for Research on Molecular Electronics and Photonics, Laboratory of Chemical and Biological Dynamics, University of Leuven, Celestijnenlaan 200D, B-3001 Leuven, Belgium, Australian Photonics Cooperative Research Centre, Laser Physics Centre, Research School of Physical Sciences and Engineering, Australian National University, Canberra, Australian Capital Territory 0200, Australia, and Research School of Chemistry, Australian National University, Canberra, Australian Capital Territory 0200, Australia

Received March 2, 2001

The syntheses of *trans*-[Ru(C═CHR)Cl(pp)$_2$]PF$_6$ (pp = dppm, R = 4-C$_6$H$_4$C≡CPh, 4-C$_6$H$_4$-CHO, 4,4′-C$_6$H$_4$C≡CC$_6$H$_4$NO$_2$, (*E*)-4,4′-C$_6$H$_4$CH═CHC$_6$H$_4$NO$_2$, 4,4′,4″-C≡CC$_6$H$_4$C≡CC$_6$H$_4$-C≡CC$_6$H$_4$NO$_2$; pp = dppe, R = 4-C$_6$H$_4$CHO, (*E*)-4,4′-C$_6$H$_4$CH═CHC$_6$H$_4$NO$_2$) and *trans*-[Ru-(C≡CR)Cl(pp)$_2$] (pp = dppm, R = 4-C$_6$H$_4$C≡CPh, 4-C$_6$H$_4$CHO, 4,4′-C$_6$H$_4$C≡CC$_6$H$_4$NO$_2$, (*E*)-4,4′-C$_6$H$_4$CH═CHC$_6$H$_4$NO$_2$, 4,4′,4″-C≡CC$_6$H$_4$C≡CC$_6$H$_4$C≡CC$_6$H$_4$NO$_2$; pp = dppe, R = 4-C$_6$H$_4$-CHO, (*E*)-4,4′-C$_6$H$_4$CH═CHC$_6$H$_4$NO$_2$) are reported, together with X-ray structural studies of *trans*-[Ru(C≡CR)Cl(pp)$_2$] (pp = dppm, R = 4-C$_6$H$_4$C≡CPh; pp = dppe, R = 4-C$_6$H$_4$CHO, (*E*)-4,4′-C$_6$H$_4$CH═CHC$_6$H$_4$NO$_2$). Cyclic voltammetric, linear optical, and quadratic and cubic nonlinear optical response data for these new complexes, together with the corresponding data for the previously reported *trans*-[Ru(C═CHR)Cl(pp)$_2$]PF$_6$ (pp = dppm, R = Ph, 4-C$_6$H$_4$-NO$_2$; pp = dppe, R = Ph, 4-C$_6$H$_4$NO$_2$) and *trans*-[Ru(C≡CR)Cl(pp)$_2$] (pp = dppm, R = Ph, 4-C$_6$H$_4$NO$_2$, (*E*)-4,4′-C$_6$H$_4$CH═CHC$_6$H$_4$NO$_2$; pp = dppe, R = Ph, 4-C$_6$H$_4$NO$_2$), are reported. Oxidation potentials for the Ru$^{II/III}$ couple increase on proceeding from the neutral alkynyl complex to the analogous cationic vinylidene complex and on introduction of an acceptor group (CHO or NO$_2$); the complexes with 4-C≡CC$_6$H$_4$NO$_2$ ligands are the most difficult to oxidize. In some instances, the Ru$^{III/IV}$ and Ru$^{I/II}$ processes have been identified together with, where relevant, nitro-centered reduction processes. The oxidized and reduced vinylidene complexes are shown to transform electrochemically into the corresponding alkynyl complexes. Optical absorption maxima undergo a red shift upon increase of acceptor strength, replacement of the coligand dppm with dppe, and replacement of the alkynyl ligand yne linkage with an ene linkage. Proceeding from the vinylidene complex to an analogous alkynyl complex results in a small red shift in absorption maximum and a significant increase in extinction coefficient. Quadratic molecular nonlinearities by hyper-Rayleigh scattering measurements at 1064 nm increase upon introduction of ligated metal (proceeding from precursor alkyne to alkynyl or vinylidene complex), an increase in acceptor strength (introduction of CHO or NO$_2$), alkynyl chain lengthening (in the series [4-C≡CC$_6$H$_4$]$_n$-4-NO$_2$, proceeding from n = 1 and 2 to 3), and replacing the yne linkage with an ene linkage. Significant differences in β value for two vinylidene/alkynyl complex pairs suggest that they could function as precursors to protically switchable quadratic NLO materials at 1064 nm. Cubic molecular nonlinearities by Z-scan measurements at 800 nm are in many cases characterized by negative real and significant imaginary components, indicative of two-photon effects; nevertheless, a substantial increase in $|\gamma|$ on proceeding to the largest molecule, *trans*-Ru(4,4′,4"-C≡CC$_6$H$_4$C≡CC$_6$H$_4$C≡CC$_6$H$_4$NO$_2$)Cl(dppm)$_2$, is observed. An order of magnitude difference in γ_{imag} values (and therefore two-photon absorption (TPA) cross sections σ_2) for vinylidene/alkynyl complex pairs suggest that they have potential as protically switchable TPA materials at 800 nm.

Introduction

The nonlinear optical (NLO) merit of organometallic complexes has attracted significant attention recently.[2−6] The quadratic and cubic NLO properties of a wide range of complex types have been assayed, with those incorporating metallocenyl or alkynylmetal units the most intensively studied. We have previously reported comprehensive structure/NLO property correlations for donor−bridge−acceptor (cyclopentadienyl)bis(phosphine)-

* To whom correspondence should be addressed. E-mail: Mark.Humphrey@anu.edu.au.
[†] Department of Chemistry, Australian National University.
[‡] University of Leuven.
[§] Laser Physics Centre, Australian National University.
[∥] Research School of Chemistry, Australian National University.

10.1021/om0101700 CCC: $20.00
Publication on Web 09/20/2001

ruthenium,[7−10] (cyclopentadienyl)(triphenylphosphine)-nickel,[10−12] and (triphenylphosphine)gold[10,11,13,14] nitroarylalkynyl complexes. Quadratic NLO merit for alkynylmetal complexes at 1064 nm increases upon increasing the metal valence electron count (progressing from 14-electron gold to analogous 18-electron nickel or ruthenium complexes) and ease of metal oxidation (progressing from less readily oxidizable nickel to more easily oxidizable ruthenium analogues). Cubic NLO merit for these complexes at 800 nm increases on progressing from 18-electron ruthenium or nickel complexes to 14-electron gold analogues. We report herein the effect upon both quadratic and cubic NLO properties of three further substantive modifications: (i) replacing the (cyclopentadienyl)bis(triphenylphosphine)ruthenium by chlorobis(diphosphine)ruthenium (diphosphine ≡ bis-(diphenylphosphino)methane (dppm), bis(diphenylphosphino)ethane (dppe)), to assess the impact of wholesale coligand variation, (ii) replacing the ubiquitous nitro acceptor group in our arylalkynyl complexes by an aldehyde functionality, a substitution which affords the longer term prospect of derivatization, and (iii) replacing the alkynyl ligand by its precursor, the vinylidene ligand, a substitution which results in an electron-deficient bridging unit and an increase in M−C π-bonding. The last-mentioned modification is significant for two reasons. First, the existence of M−C π-bonding is a suggested organometallic NLO material design criterion[15] which has been little studied.[16−18] Second, electrochemical switching of quadratic NLO output is of significant current interest,[19−21] but other possibilities for switching response in inorganic complexes have not been actively studied. For the current series of complexes, the facile interconversion of alkynyl and vinylidene ligands by protonation/deprotonation sequences may offer a route into pH switching of both the quadratic and cubic NLO response.

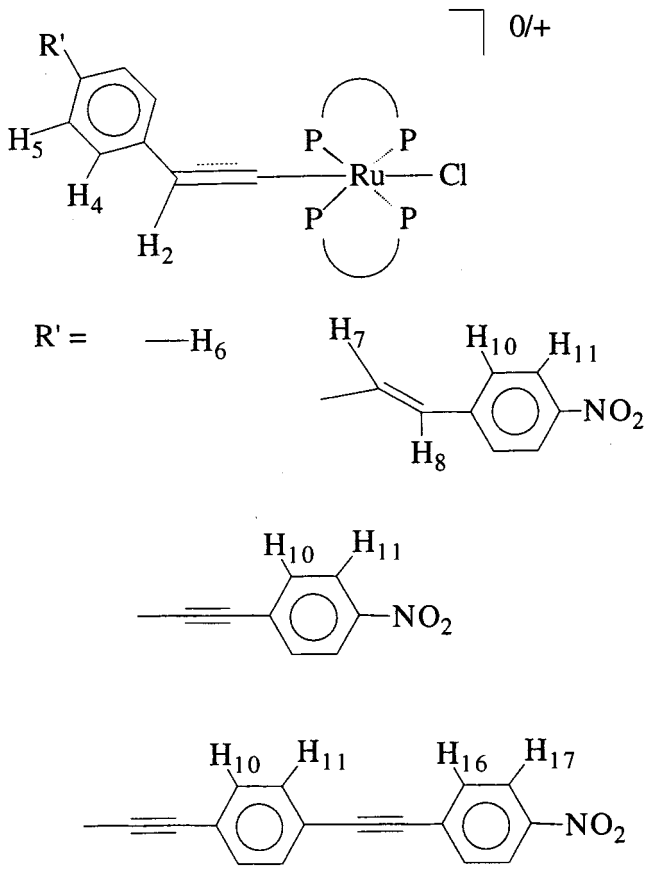

Figure 1. NMR labeling scheme.

Experimental Section

General Information. Reactions were carried out using standard Schlenk techniques,[22] under a nitrogen atmosphere. The solvents Et_2O, CH_2Cl_2, tetrahydrofuran (thf). and NEt_3 were dried according to standard procedures; other solvents and reagents were obtained from Aldrich and used as received. Column chromatography was on Merck silica gel 60 (70−230 ASTM) or Merck alumina oxide 90 active basic (activity grade II, 70−230 mesh ASTM). The term "petrol" refers to a fraction of petroleum ether with a boiling range of 60−80 °C.

Microanalyses were carried out at the Australian National University. Infrared spectra were recorded using a Perkin-Elmer System 2000 FT-IR spectrometer as CH_2Cl_2 solutions using CaF_2 cells unless otherwise stated. UV−vis spectra were recorded on a Cary 5 spectrometer as thf solutions. ^1H (300 MHz) and $^{31}P\{^1H\}$ (121 MHz) NMR spectra were recorded using a Varian Gemini-300 or VXR-300 NMR spectrometer in $CDCl_3$ unless otherwise stated and were referenced to residual solvent and to external 85% H_3PO_4 (0.0 ppm), respectively. The numbering scheme for spectral assignments is given in Figure 1. Secondary ion (SI) mass spectra were recorded on a VG ZAB 2SEQ spectrometer (30 kV Cs^+ ions, current 1 mA, accelerating potential 8 kV, matrix 3-nitrobenzyl alcohol) and electron

(1) McDonagh, A. M.; Cifuentes, M. P.; Humphrey, M. G.; Houbrechts, S.; Persoons, A. *J. Organomet. Chem.* **2000**, *610*, 71.
(2) Nalwa, H. S. *Appl. Organomet. Chem.* **1991**, *5*, 349.
(3) *Inorganic Materials*; Marder, S. R., Ed.; Wiley: New York, 1992; p 116.
(4) Long, N. J. *Angew. Chem., Int. Ed. Engl.* **1995**, *34*, 21.
(5) Whittall, I. R.; McDonagh, A. M.; Humphrey, M. G.; Samoc, M. *Adv. Organomet. Chem.* **1998**, *42*, 291.
(6) Whittall, I. R.; McDonagh, A. M.; Humphrey, M. G.; Samoc, M. *Adv. Organomet. Chem.* **1999**, *43*, 349.
(7) Whittall, I. R.; Humphrey, M. G.; Persoons, A.; Houbrechts, S. *Organometallics* **1996**, *15*, 1935.
(8) Whittall, I. R.; Humphrey, M. G.; Samoc, M.; Swiatkiewicz, J.; Luther-Davies, B. *Organometallics* **1995**, *14*, 5493.
(9) Whittall, I. R.; Cifuentes, M. P.; Humphrey, M. G.; Luther-Davies, B.; Samoc, M.; Houbrechts, S.; Persoons, A.; Heath, G. A.; Hockless, D. C. R. *J. Organomet. Chem.* **1997**, *549*, 127.
(10) Naulty, R. H.; Cifuentes, M. P.; Humphrey, M. G.; Houbrechts, S.; Boutton, C.; Persoons, A.; Heath, G. A.; Hockless, D. C. R.; Luther-Davies, B.; Samoc, M. *J. Chem. Soc., Dalton Trans.* **1997**, 4167.
(11) Whittall, I. R.; Humphrey, M. G.; Houbrechts, S.; Maes, J.; Persoons, A.; Schmid, S.; Hockless, D. C. R. *J. Organomet. Chem* **1997**, *544*, 277.
(12) Whittall, I. R.; Cifuentes, M. P.; Humphrey, M. G.; Luther-Davies, B.; Samoc, M.; Houbrechts, S.; Persoons, A.; Heath, G. A.; Bogsanyi, D. *Organometallics* **1997**, *16*, 2631.
(13) Whittall, I. R.; Humphrey, M. G.; Samoc, M.; Luther-Davies., B. *Angew. Chem., Int. Ed. Engl.* **1997**, *36*, 370.
(14) Whittall, I. R.; Humphrey, M. G.; Houbrechts, S.; Persoons, A.; Hockless, D. C. R. *Organometallics* **1996**, *15*, 5738.
(15) Calabrese, J. C.; Cheng, L.-T.; Green, J. C.; Marder, S. R.; Tam, W. *J. Am. Chem. Soc.* **1991**, *113*, 7227.
(16) Cadierno, V.; Conejero, S.; Gamasa, M. P.; Gimeno, J.; Asselberghs, I.; Houbrechts, S.; Clays, K.; Persoons, A.; Borge, J.; García-Granda, S. *Organometallics* **1999**, *18*, 582.
(17) Whittall, I. R.; Cifuentes, M. P.; Costigan, M. J.; Humphrey, M. G.; Goh, S. C.; Skelton, B. W.; White, A. H. *J. Organomet. Chem.* **1994**, *471*, 193.
(18) Cifuentes, M. P.; Driver, J.; Humphrey, M. G.; Asselberghs, I.; Persoons, A.; Samoc, M.; Luther-Davies, B. *J. Organomet. Chem.* **2000**, *607*, 72.
(19) Coe, B. J.; Houbrechts, S.; Asselberghs, I.; Persoons, A. *Angew. Chem., Int. Ed.* **1999**, *38*, 366.
(20) Coe, B. J. *Chem. Eur. J.* **1999**, *5*, 2464.
(21) Malaun, M.; Reeves, Z. R.; Paul, R. L.; Jeffery, J. C.; McCleverty, J. A.; Ward, M. D.; Asselberghs, I.; Clays, K.; Persoons, A. *Chem. Commun.* **2001**, 49.
(22) Shriver, D. F.; Drezdzon, M. A. *The Manipulation of Air-Sensitive Compounds*, 2nd ed.; Wiley-Interscience: Chichester, U.K., 1986.

impact (EI), including high resolution (HR), mass spectra on a VG Autospec instrument (70 eV electron energy, 8 kV accelerating potential) at the Australian National University; peaks are reported as *m/z* (assignment, relative intensity). Electrochemical measurements were recorded on a MacLab 400 interface and MacLab potentiostat from ADInstruments using a platinum-disk working electrode, a Pt auxiliary electrode, and Ag−AgCl reference minielectrodes from Cypress Systems. Scan rates were typically 100 mV s^{-1}. Solutions contained 0.1 M $NBu^n_4PF_6$ and ca. 10^{-3} M complex in CH_2Cl_2. Solutions were purged and maintained under an atmosphere of nitrogen. All values are referenced to an internal ferrocene/ferrocenium couple at 0.56 V. The following were prepared by following literature procedures: 4-HC≡CC_6H_4C≡CPh (**1**),[23] 4-HC≡$CC_6H_4NO_2$ (**2**),[24] 4,4′-HC≡CC_6H_4C≡$CC_6H_4NO_2$ (**3**),[23] 4-HC≡CC_6H_4CHO (**7**),[25] 4-Me_3SiC≡CC_6H_4I,[26] $PdCl_2(PPh_3)_2$,[27] *cis*-[$RuCl_2$(pp)$_2$] (pp = dppm (**8**), dppe (**10**)),[28] *trans*-[$RuCl_2$(pp)$_2$] (pp = dppm (**9**), dppe (**11**)),[29] *trans*-[Ru(C=CHPh)Cl(dppm)$_2$]-PF_6 (**12**),[30] *trans*-[Ru(C≡CPh)Cl(dppm)$_2$] (**13**), *trans*-[Ru-(4-C≡$CC_6H_4NO_2$)Cl(dppm)$_2$] (**19**), and *trans*-[Ru{(*E*)-4,4′-C≡CC_6H_4CH=$CHC_6H_4NO_2$}Cl(dppm)$_2$] (**25**),[31] *trans*-[Ru(4-C=$CHC_6H_4NO_2$)Cl(dppm)$_2$]PF_6 (**18**),[32] *trans*-[Ru(4-C=CHC_6H_4R)-Cl(dppe)$_2$]PF_6 (R = H (**26**), NO_2 (**30**)), and *trans*-[Ru(4-C≡CC_6H_4R)Cl(dppe)$_2$] (R = H (**27**), NO_2 (**31**)).[33]

Synthesis of (*E*)-4,4′-HC≡CC_6H_4CH=$CHC_6H_4NO_2$ (4). The following modification to the published procedure[7,34] afforded the *E* stereoisomer selectively in excellent yield. 4-Nitrobenzyl bromide (2.0 g, 9.2 mmol) was placed in a flask equipped with an air condenser and heated for 1 h in refluxing triethyl phosphite (1.6 mL, 9.2 mmol). The resultant mixture was cooled to room temperature. A solution of NaOMe (240 mg, 9.4 mmol) in dimethylformamide (5 mL) was then added, and the resultant solution was stirred for 5 min at 0 °C. To this solution was slowly added 4-HC≡CC_6H_4CHO (1.2 g, 9.0 mmol), and the resultant mixture was stirred for 5 min at 0 °C and then for 10 min at room temperature. H_2O (5 mL) and MeOH (2 mL) were added to the solution to afford a yellow precipitate, which was collected, washed (H_2O, MeOH), and dried in vacuo to afford **4** as a yellow solid (1.2 g, 85%) by comparison with the published spectral data.

Synthesis of 4,4′,4″-Me_3SiC≡CC_6H_4C≡CC_6H_4C≡$CC_6H_4NO_2$ (5). A mixture of 4,4′-HC≡CC_6H_4C≡$CC_6H_4NO_2$ (**3**, 100 mg, 0.31 mmol), 4-Me_3SiC≡CC_6H_4I (113 mg, 0.38 mmol), $PdCl_2(PPh_3)_2$ (15.0 mg), and CuI (5.0 mg) in NEt_3 (50 mL) was stirred at 35 °C for 3 h. The solvent was removed under reduced pressure and the solid extracted with CH_2Cl_2 (40 mL) and water (2 × 40 mL**)**. The organic fraction was collected and dried with $MgSO_4$. Filtration followed by column chromatography on alumina afforded a pale yellow band on elution with 3:2 petrol/CH_2Cl_2. The band was collected and the solvent removed to afford a pale yellow solid, which was recrystallized from CH_2Cl_2/MeOH and identified as **5** (103 mg, 78%). Anal. Calcd for $C_{27}H_{21}NO_2Si·0.5CH_3OH$: C, 75.84; H, 5.32; N, 3.22. Found: C, 76.07, H, 5.27, N, 3.25. IR: ν(C≡C) 2157 w cm^{-1}. UV−vis: λ 346 nm, ϵ 5.0×10^4 M^{-1} cm^{-1}. ^{1}H NMR: δ 0.24 (s, 9H, $SiMe_3$), 3.48 (s, 1.5H, CH_3OH), 7.44 (s, 4H, H_4, H_5), 7.52 (s, 4H, H_{10}, H_{11}), 7.65 (d, 2H, J_{HH} = 8 Hz, H_{16}), 8.21 (d, 2H, J_{HH} = 8 Hz, H_{17}). EI MS: 419 ([M]$^+$, 100), 404 ([M − Me]$^+$, 90), 389 ([M − 2Me]$^+$, 15), 358 ([M − Me − NO_2]$^+$, 20). HR MS: calcd for $C_{27}H_{21}NO_2Si$ *m/z* 419.1343, found 419.1342.

Synthesis of 4,4′,4″-HC≡CC_6H_4C≡CC_6H_4C≡$CC_6H_4NO_2$ (6). NBu^n_4F (2 mL, 1 M solution in thf) was added to a solution of 4,4′,4″-Me_3SiC≡CC_6H_4C≡CC_6H_4C≡$CC_6H_4NO_2$ (**5**; 80 mg, 0.19 mmol) in CH_2Cl_2 (15 mL), and the solution was stirred for 30 min. The mixture was filtered through an alumina plug (15 cm^3). Addition of petrol (25 mL) followed by removal of the solvent under reduced pressure afforded **6** as a pale yellow solid (55 mg, 83%). Anal. Calcd for $C_{24}H_{13}NO_2$: C, 82.98; H, 3.77; N, 4.03. Found: C, 82.62; H, 3.97; N, 4.07. IR: ν(HC≡) 3301w, ν(C≡C) 2109 w cm^{-1}. UV−vis: λ 351 nm, ϵ 5.2×10^4 M^{-1} cm^{-1}. ^{1}H NMR: δ 3.17 (s, 1H, C≡CH), 7.44 (s, 4H, H_4, H_5), 7.52 (s, 4H, H_{10}, H_{11}), 7.65 (d, 2H, J_{HH} = 9 Hz, H_{16}), 8.22 (d, 2H, J_{HH} = 9 Hz, H_{17}). EI MS: 347 ([M]$^+$, 100), 300 ([M − NO_2 − H]$^+$, 20). HR MS: calcd for $C_{24}H_{13}NO_2$ *m/z* 347.0943, found 347.0946.

Synthesis of *trans*-[Ru(4-C=CHC_6H_4C≡CPh)Cl(dppm)$_2$]-PF_6 (14). *cis*-[$RuCl_2$(dppm)$_2$] (**8**; 400 mg, 0.43 mmol), NH_4PF_6 (140 mg, 0.86 mmol), and 4-HC≡CC_6H_4C≡CPh (**1**; 174 mg, 0.86 mmol) were added to CH_2Cl_2 (25 mL), and the mixture was refluxed for 2 h. Addition of petrol (50 mL) to the cooled reaction mixture afforded a precipitate which was collected and washed with Et_2O, to afford **14** as a salmon pink solid (410 mg, 76%). Anal. Calcd for $C_{66}H_{54}ClF_6P_5Ru$: C, 63.29; H, 4.34. Found: C, 63.33; H, 4.66. IR: ν(C≡C) 2064 m, ν(PF) 837 s cm^{-1}. UV−vis: λ 381 nm, ϵ 2.1×10^4 M^{-1} cm^{-1}. ^{1}H NMR: δ 3.05 (m, 1H, =CH), 5.12 (m, 2H, PCH_2), 5.32 (m, 2H, PCH_2), 5.45 (d, J_{HH} = 8 Hz, 2H, H_4), 6.02 (d, J_{HH} = 8 Hz, 2H, H_5), 6.77 (d, J_{HH} = 8 Hz, 2H, H_{10}), 6.87 (d, J_{HH} = 8 Hz, 2H, H_{11}), 7.10−7.60 (m, 41H, H_{12} + Ph). ^{31}P NMR: δ −15.6. SI MS: 1107 ([M − PF_6]$^+$, 60), 1071 ([M − HCl − PF_6]$^+$, 10), 904 ([M − C=CHC_6H_4C≡CPh − PF_6]$^+$, 100), 869 ([Ru(dppm)$_2$ − H]$^+$, 80).

Synthesis of *trans*-[Ru(4-C≡CC_6H_4C≡CPh)Cl(dppm)$_2$] (15). A mixture of **14** (200 mg, 0.17 mmol) and NEt_3 (1.0 mL) was stirred in CH_2Cl_2 (25 mL) for 10 min and then passed through an alumina plug. Petrol (50 mL) was added and the resulting precipitate collected and washed with petrol to afford **15** as a yellow solid (160 mg, 83%). Crystals suitable for the X-ray study were grown by solvent diffusion of MeOH into a CH_2Cl_2 solution of **15**. Anal. Calcd for $C_{66}H_{53}ClP_4Ru·0.5CH_2Cl_2$: C, 69.51; H, 4.47. Found: C, 69.63; H, 4.28. IR: ν(C≡C) 2066 m cm^{-1}. UV−vis: λ 380 nm, ϵ 2.9×10^4 M^{-1} cm^{-1}. ^{1}H NMR: δ 4.89 (m, 2H, PCH_2), 5.28 (s, 1H, CH_2Cl_2), 5.63 (m, 2H, PCH_2), 6.02 (d, J_{HH} = 8 Hz, 2H, H_4), 6.78 (d, J_{HH} = 8 Hz, 2H, H_5), 7.10−7.60 (m, 45H, Ph). ^{31}P NMR: δ −15.2. SI MS: 1106 ([M]$^+$, 100), 905 ([M − C≡CC_6H_4C≡CPh]$^+$, 25), 869 ([Ru(dppm)$_2$ − H]$^+$, 40), 483 ([Ru(dppm)]$^+$, 30).

Synthesis of *trans*-[Ru(4-C=CHC_6H_4CHO)Cl(dppm)$_2$]-PF_6 (16). *cis*-[$RuCl_2$(dppm)$_2$] (**8**; 300 mg, 0.32 mmol), NH_4PF_6 (105 mg, 0.64 mmol), and 4-HC≡CC_6H_4CHO (83 mg, 0.64 mmol) were added to CH_2Cl_2 (25 mL), and the mixture was stirred for 6 h. The cooled reaction mixture was passed through a sintered-glass funnel to remove NH_4Cl and excess NH_4PF_6. The solvent was removed under reduced pressure, and the resulting residue was washed with Et_2O, affording **16** as an orange-yellow powder (240 mg, 73%). Anal. Calcd for $C_{59}H_{50}ClF_6OP_5Ru$: C, 60.03; H, 4.27. Found: C, 60.34; H, 4.33. IR (KBr): ν(PF) 838 s cm^{-1}. UV−vis: λ 403 nm, ϵ 1.9×10^4 M^{-1} cm^{-1}. ^{1}H NMR: δ 3.17 (m, 1H, =CH), 5.25 (m, 4H, PCH_2), 5.62 (d, J_{HH} = 8 Hz, 2H, H_4), 7.10−7.55 (m, 42H, H_5 + Ph), 9.75 (s, 1H, CHO). ^{31}P NMR: δ −16.1. SI MS: 1035 ([M − PF_6]$^+$, 95),

(23) Lavastre, O.; Cabioch, S.; Dixneuf, P. H.; Vohlidal, J. *Tetrahedron* **1997**, *53*, 7595.
(24) Takahashi, S.; Kuroyama, Y.; Sonogashira, K.; Hagihara, N. *Synthesis* **1980**, 627.
(25) Austin, W. B.; Bilow, N.; Kelleghan, W. J.; Lau, K. S. Y. *J. Org. Chem.* **1981**, *46*, 2280.
(26) Hsung, P.; Chidsey, C. E. D.; Sita, L. R. *Organometallics* **1995**, *14*, 4808.
(27) Khan, M. S.; Schwartz, D. J.; Pasha, N. A.; Kakkar, A. K.; Lin, B.; Raithby, P. R.; Lewis, J. *Z. Anorg. Allg. Chem.* **1992**, *616*, 121.
(28) Chaudret, B.; Commenges, G.; Poilblanc, R. *J. Chem. Soc., Dalton Trans.* **1984**, 1635.
(29) Chatt, J.; Hayter, R. G. *J. Chem. Soc., Dalton Trans.* **1961**, 896.
(30) Touchard, D.; Haquette, P.; Pirio, N.; Toupet, L.; Dixneuf, P. H. *Organometallics* **1993**, *12*, 3132.
(31) McDonagh, A. M.; Whittall, I. R.; Humphrey, M. G.; Skelton, B. W.; White, A. H. *J. Organomet. Chem.* **1996**, *519*, 229.
(32) Hodge, A. J.; Ingham, S. L.; Kakkar, A. K.; Khan, M. S.; Lewis, J.; Long, N. J.; Parker, D. G.; Raithby, P. R. *J. Organomet. Chem.* **1995**, *488*, 205.
(33) Touchard, D.; Haquette, P.; Guesmi, S.; Pichon, L. L.; Daridor, A.; Toupet, L.; Dixneuf, P. H. *Organometallics* **1997**, *16*, 3640.
(34) Hockless, D. C. R.; Whittall, I. R.; Humphrey, M. G. *Acta Crystallogr., Sect. C: Cryst. Struct. Commun.* **1996**, *52*, 3222.

999 ([M − PF_6 − HCl]$^+$, 20), 905 ([M − PF_6 − C═CHC_6H_4-CHO]$^+$, 90), 869 ([Ru(dppm)$_2$ − H]$^+$, 100), 485 ([Ru(dppm) − H]$^+$, 55).

Synthesis of *trans*-[Ru(4-C≡CC_6H_4CHO)Cl(dppm)$_2$] (17). *cis*-[$RuCl_2$(dppm)$_2$] (**8**; 300 mg, 0.32 mmol), NH_4PF_6 (105 mg, 0.64 mmol), and 4-HC≡CC_6H_4CHO (83 mg, 0.64 mmol) were added to CH_2Cl_2 (25 mL), and the mixture was stirred for 6 h. NEt_3 (0.5 mL) and petrol (10 mL) were added, and the mixture was passed through a silica plug. The solvents were removed under reduced pressure, and the resulting residue was purified by column chromatography on alumina using 1:1 CH_2Cl_2/petrol as eluant. The major, yellow, band was collected and the solvent removed to afford **17** as a yellow solid (220 mg, 66%). Anal. Calcd for $C_{59}H_{49}ClOP_4Ru\cdot 0.75CH_2Cl_2$: C, 65.35; H, 4.64. Found: C, 65.27; H 4.91. IR: ν(C≡C) 2059 m cm^{-1}. UV−vis: λ 405 nm, ϵ 6.0 × 10^4 M^{-1} cm^{-1}. ^{1}H NMR: δ 4.92 (m, 4H, PCH_2), 5.28 (s, 1.5H, CH_2Cl_2), 6.03 (d, J_{HH} = 8 Hz, 2H, H_4), 7.00−7.60 (m, 42H, H_5 + Ph), 9.75 (s, 1H, CHO). ^{31}P NMR: δ −5.9. SI MS: 1034 ([M]$^+$, 100), 999 ([M − Cl]$^+$, 12), 905 ([M − C≡CC_6H_4CHO]$^+$, 6), 869 ([Ru(dppm)$_2$ − H]$^+$, 12), 486 ([Ru(dppm)]$^+$, 75).

Synthesis of *trans*-[Ru(4,4′−C═CHC_6H_4C≡$CC_6H_4NO_2$)Cl(dppm)$_2$]PF_6 (20). A mixture of *cis*-[$RuCl_2$(dppm)$_2$] (**8**; 400 mg, 0.43 mmol), NH_4PF_6 (140 mg, 0.86 mmol), and 4,4′-HC≡CC_6H_4C≡$CC_6H_4NO_2$ (**3**; 210 mg, 0.86 mmol) in CH_2Cl_2 (25 mL) was refluxed for 2 h. Petrol (50 mL) was added to the cooled solution, and the resulting precipitate was collected and washed with Et_2O to afford **20** as a yellow-orange solid (440 mg, 79%). Anal. Calcd for $C_{66}H_{53}ClNO_2P_5F_6Ru$: C, 61.10; H, 4.12; N, 1.08. Found: C, 61.68; H, 4.48; N, 1.34. IR (KBr): ν(C≡C) 2069 m, ν(PF) 836 s cm^{-1}. UV−vis: λ 461 nm, ϵ 1.2 × 10^4 M^{-1} cm^{-1}. ^{1}H NMR: δ 3.08 (m, 1H, ═CH), 5.15 (m, 2H, PCH_2), 5.34 (m, 2H, PCH_2), 5.50 (d, J_{HH} = 8 Hz, 2H, H_4), 6.89 (d, J_{HH} = 8 Hz, 2H, H_5), 7.10−7.50 (m, 40H, Ph), 7.64 (d, J_{HH} = 9 Hz, 2H, H_{10}), 8.20 (d, J_{HH} = 9 Hz, 2H, H_{11}). ^{31}P NMR: δ −15.8. SI MS: 1152 ([M − PF_6]$^+$, 20), 1117 ([M − Cl − PF_6]$^+$, 65), 905 ([M − C═CHC_6H_4C≡$CC_6H_4NO_2$ − PF_6]$^+$, 45), 869 ([Ru(dppm)$_2$ − H]$^+$, 60), 485 ([Ru(dppm) − H]$^+$, 40).

Synthesis of *trans*-[Ru(4,4′−C≡CC_6H_4C≡$CC_6H_4NO_2$)Cl(dppm)$_2$] (21). A solution of **20** (200 mg, 0.15 mmol) and NEt_3 (1.0 mL) in CH_2Cl_2 (25 mL) was stirred for 10 min. The mixture was then passed through an alumina plug, petrol (50 mL) was added, and the resulting precipitate was washed with petrol to afford **21** as a red solid (140 mg, 83%). Anal. Calcd for $C_{66}H_{52}ClNO_2P_4Ru$: C, 68.84; H, 4.55; N, 1.21. Found: C, 68.14; H, 4.62; N 1.21. IR (KBr): ν(C≡C) 2064 m, 2059 s cm^{-1}. UV−vis: λ 468 nm, ϵ 2.3 × 10^4 M^{-1} cm^{-1}. ^{1}H NMR: δ 4.90 (m, 4H, PCH_2P), 5.97 (d, J_{HH} = 8 Hz, 2H, H_4), 7.00−7.50 (m, 42H, H_5 + Ph), 7.57 (d, J_{HH} = 9 Hz, 2H, H_{10}), 8.18 (d, J_{HH} = 9 Hz, 2H, H_{11}). ^{31}P NMR: δ −5.8. SI MS: 1151 ([M]$^+$, 100), 905 ([M − C≡CC_6H_4C≡$CC_6H_4NO_2$]$^+$, 20), 869 ([Ru(dppm)$_2$ − H]$^+$, 60), 486 ([Ru(dppm)]$^+$, 30).

Synthesis of *trans*-[Ru(4,4′,4″−C═CHC_6H_4C≡CC_6H_4C≡$CC_6H_4NO_2$)Cl(dppm)$_2$]PF_6 (22). *cis*-[$RuCl_2$(dppm)$_2$] (**8**; 100 mg, 0.11 mmol), NH_4PF_6 (36 mg, 0.22 mmol), and 4,4′,4″-HC≡CC_6H_4C≡CC_6H_4C≡$CC_6H_4NO_2$ (**6**; 44 mg, 0.13 mmol) were stirred in CH_2Cl_2 (25 mL) for 3 h. The mixture was filtered, petrol (50 mL) was added, and the resulting precipitate was collected and washed with Et_2O to afford **22** as a red solid (108 mg, 73%). Anal. Calcd for $C_{74}H_{57}ClF_6NO_2P_5Ru\cdot 0.5CH_2Cl_2$: C, 62.14; H, 4.06; N, 0.97. Found: C, 62.39; H, 4.67; N, 1.05. IR: ν(C≡C) 2211 s, 2065 m, ν(PF) 838 s cm^{-1}. UV−vis: λ 427 nm, ϵ 1.4 × 10^4 M^{-1} cm^{-1}. ^{1}H NMR: δ 3.05 (m, 1H, H_2), 5.13 (m, 2H, PCH_2P), 5.28 (s, 1H, CH_2Cl_2), 5.34 (m, 2H, PCH_2P), 5.48 (d, J_{HH} = 8 Hz, 2H, H_4), 6.90−7.55 (m, 46H, Ph), 7.65 (d, J_{HH} = 9 Hz, 2H, H_{10}), 8.21 (d, J_{HH} = 9 Hz, 2H, H_{11}). ^{31}P NMR: δ −15.9. SI MS: 1252 ([M − PF_6]$^+$, 15), 905 ([RuCl(dppm)$_2$]$^+$, 90), 871 ([Ru(dppm)$_2$ + H]$^+$, 100).

Synthesis of *trans*-[Ru(4,4′,4″−C≡CC_6H_4C≡CC_6H_4C≡$CC_6H_4NO_2$)Cl(dppm)$_2$] (23). A solution of *trans*-[Ru(4,4′,4″−C═CHC_6H_4C≡CC_6H_4C≡$CC_6H_4NO_2$)Cl(dppm)$_2$]PF_6 (**22**; 100 mg, 0.072 mmol) and NEt_3 (1 mL) in CH_2Cl_2 (25 mL) was stirred for 10 min at room temperature. The mixture was passed through an alumina plug (10 cm^3), and petrol (50 mL) was added to the filtrate to afford a red precipitate. This was collected and washed with petrol to afford **23** as a red solid (78 mg, 87%). Anal. Calcd for $C_{74}H_{56}ClNO_2P_4Ru\cdot CH_2Cl_2$: C, 67.40; H, 4.37; N, 1.05. Found: C, 67.71; H, 4.68; N, 1.25. IR: ν(C≡C) 2205 m, 2070 s cm^{-1}. UV−vis: λ 439 nm, ϵ 2.0 × 10^4 M^{-1} cm^{-1}. ^{1}H NMR: δ 4.90 (m, 4H, PCH_2), 5.28 (s, 2H, CH_2Cl_2), 5.97 (d, J_{HH} = 8 Hz, 2H, H_4), 7.00−7.50 (m, 48H, Ph), 8.22 (d, J_{HH} = 9 Hz, 2H, H_{17}). ^{31}P NMR: δ −6.0. SI MS: 1252 ([M + H]$^+$, 100), 869 ([Ru(dppm)$_2$ − H]$^+$, 90), 485 ([Ru(dppm) − H]$^+$, 90).

Synthesis of *trans*-[Ru{(*E*)-4,4′-C═CHC_6H_4CH═$CHC_6H_4NO_2$}Cl(dppm)$_2$]PF_6 (24). *cis*-[$RuCl_2$(dppm)$_2$] (**8**; 200 mg, 0.21 mmol), (*E*)-4,4′-HC≡CC_6H_4CH═$CHC_6H_4NO_2$ (**4**; 80 mg, 0.32 mmol) and $NaPF_6$ (35 mg, 0.21 mmol) were stirred in CH_2Cl_2 (15 mL) for 3 h. Petrol (50 mL) was then added and the resultant precipitate washed with Et_2O to afford **24** as a red solid (200 mg, 72%). Anal. Calcd for $C_{66}H_{55}ClF_6NO_2P_5Ru\cdot 0.5CH_2Cl_2$: C, 59.51; H, 4.21; N, 1.04. Found: C, 59.34; H, 4.50; N, 1.12. IR: ν(C═C) 1625 m, v(PF) 847 s cm^{-1}. UV−vis: λ 436 (sh) nm, ϵ 0.64 × 10^4 M^{-1} cm^{-1}. ^{1}H NMR: δ 3.08 (m, 1H, ═CH), 5.27 (m, 4H, PCH_2), 5.28 (s, 1H, CH_2Cl_2), 5.56 (d, J_{HH} = 4 Hz, 2H, H_4), 6.75 (d, J_{HH} = 4 Hz, 2H, H_5), 6.90−7.45 (42H, H_{78} + Ph), 7.59 (d, J_{HH} = 6 Hz, 2H, H_{10}), 8.17 (d, J_{HH} = 6 Hz, 2H, H_{11}). ^{31}P NMR: δ −15.6. SI MS: 1154 ([M − PF_6]$^+$, 47), 905 ([RuCl(dppm)$_2$]$^+$, 100), 869 ([Ru(dppm)$_2$ − H]$^+$, 60).

Synthesis of *trans*-[Ru(4-C═CHC_6H_4CHO)Cl(dppe)$_2$]PF_6 (28). A mixture of *cis*-[$RuCl_2$(dppe)$_2$] (**10**; 300 mg, 0.31 mmol), NH_4PF_6 (101 mg, 0.62 mmol), and 4-HC≡CC_6H_4CHO (**7**; 83 mg, 0.64 mmol) in CH_2Cl_2 (25 mL) was stirred for 6 h and was then filtered to remove NH_4Cl and excess NH_4PF_6. The solvent was removed under reduced pressure, and the resulting residue was washed with Et_2O to afford **28** as a yellow solid (375 mg, 78%). Anal. Calcd for $C_{61}H_{54}ClF_6OP_5Ru$: C, 60.63; H, 4.50. Found: C, 60.43; H 4.77. IR (KBr): ν(PF) 836s cm^{-1}. UV−vis: λ 413 nm, ϵ 2.0 × 10^4 M^{-1} cm^{-1}. ^{1}H NMR: δ 2.70−3.10 (m, 8H, PCH_2), 4.47 (m, 1H, ═CH), 5.70 (d, 2H, H_4), 6.90−7.40 (m, 42H, H_5 + Ph), 9.64 (s, 1H, CHO). ^{31}P NMR: δ 35.9. SI MS: 1063 ([M − PF_6]$^+$, 100), 1027 ([M − PF_6 − HCl]$^+$, 30), 933 ([M − PF_6 − C═CHC_6H_4CHO]$^+$, 40), 897 ([Ru(dppe)$_2$ − H]$^+$, 45), 498 ([Ru(dppe) − 2H]$^+$, 98).

Synthesis of *trans*-[Ru(4-C≡CC_6H_4CHO)Cl(dppe)$_2$] (29). A mixture of *cis*-[$RuCl_2$(dppe)$_2$] (**10**; 300 mg, 0.31 mmol), NH_4PF_6 (101 mg, 0.64 mmol), and 4-HC≡CC_6H_4CHO (**7**; 81 mg, 0.64 mmol) in CH_2Cl_2 (25 mL) was stirred for 6 h. NEt_3 (0.5 mL) and petrol (10 mL) were then added, and the mixture was passed through an alumina plug (10 cm^3). The solvent was removed from the filtrate under reduced pressure, and the resulting residue was washed with Et_2O, taken up in CH_2Cl_2, and purified by column chromatography using 1:1 CH_2Cl_2/petrol as eluant. The major yellow band was collected and taken to dryness to afford **29** as a yellow solid (230 mg, 70%). Recrystallization by solvent diffusion of MeOH into a CH_2Cl_2 solution afforded yellow crystals suitable for the X-ray study. Anal. Calcd for $C_{61}H_{53}ClOP_4Ru\cdot 1.75CH_2Cl_2$: C, 62.23; H, 4.70. Found: C, 62.60; H 4.53. IR: ν(C≡C) 2047 m cm^{-1}. UV−vis: λ 413 nm, ϵ 2.8 × 10^4 M^{-1} cm^{-1}. ^{1}H NMR: δ 2.66 (m, 8H, PCH_2), 5.28 (s, 3.5H, CH_2Cl_2), 6.57 (d, 2H, J_{HH} = 8 Hz, H_4), 6.90−7.40 (m, 40H, Ph), 7.57 (d, 2H, J_{HH} = 8 Hz, H_5), 9.85 (s, 1H, CHO). ^{31}P NMR: δ 49.6. SI MS: 1062 ([M]$^+$, 100), 1027 ([M − Cl]$^+$, 45), 933 ([M − C≡CC_6H_4CHO]$^+$, 8), 897 ([Ru(dppe)$_2$ − H]$^+$, 35), 498 ([Ru(dppe) − 2H]$^+$, 25).

Synthesis of *trans*-[Ru{(*E*)-4,4′-C═CHC_6H_4CH═$CHC_6H_4NO_2$}Cl(dppe)$_2$]PF_6 (32). A mixture of *cis*-[$RuCl_2$-(dppe)$_2$] (**10**; 250 mg, 0.26 mmol), (*E*)-4,4′-HC≡CC_6H_4CH═$CHC_6H_4NO_2$ (**4**; 96 mg, 0.39 mmol), and $NaPF_6$ (43 mg, 0.26 mmol) was stirred in CH_2Cl_2 (15 mL) for 3 h. Petrol (50 mL) was then added and the resultant precipitate collected and washed with Et_2O, to afford **32** as an orange powder (270 mg,

Table 1. Crystallographic Data for *trans*-[Ru(4-C≡CC$_6$H$_4$C≡CPh)Cl(dppm)$_2$] (15), *trans*-[Ru(4-C≡CC$_6$H$_4$CHO)Cl(dppe)$_2$] (29), and *trans*-[Ru{(*E*)-4,4′-C≡CC$_6$H$_4$CH=CHC$_6$H$_4$NO$_2$}Cl(dppe)$_2$] (33)

	15	29	33
empirical formula	$C_{66}H_{53}ClP_4Ru$	$C_{61}H_{53}ClOP_4Ru\cdot1.75CH_2Cl_2$	$C_{68}H_{58}ClNO_2P_4Ru\cdot0.5CH_2Cl_2$
mol wt	1106.56	1211.14	1224.10
cryst color, habit	orange, plate	yellow, needle	red, needle
cryst dimens (mm)	0.41 × 0.16 × 0.05	0.51 × 0.20 × 0.11	0.23 × 0.08 × 0.07
space group	$P2_1/n$ (No. 14)	$P\bar{1}$ (No. 2)	$P\bar{1}$ (No. 2)
a (Å)	21.173(2)	9.332(2)	12.828(2)
b (Å)	11.348(3)	13.002(3)	13.390(2)
c (Å)	24.742(3)	23.879(9)	18.949(2)
α (deg)		93.71(3)	88.90(1)
β (deg)	110.146(7)	93.95(3)	85.00(1)
γ (deg)		99.47(2)	63.493(9)
V (Å^3)	5581(2)	2842(1)	2900.9(7)
Z	4	2	2
D_{calcd} (g cm^{-3})	1.317	1.415	1.401
transmissn factors	0.49−0.83	0.88−0.94	0.67−0.73
μ (cm^{-1})	41.05 (Cu Kα)	6.41 (Mo Kα)	44.49 (Cu Kα)
N	8785	13 127	8632
N_o ($I > 2.0\sigma(I)$)	4502	8374	6630
no. of variables	649	658	706
R	0.049	0.042	0.046
R_w	0.057	0.048	0.063

79%). Anal. Calcd for $C_{68}H_{59}ClF_6NO_2P_5Ru\cdot CH_2Cl_2$: C, 58.67; H, 4.35; N, 0.99. Found: C, 58.38; H, 4.32; N, 1.27. IR: ν(C≡C) 1632, ν(PF) 847 s cm^{-1}. UV−vis: λ 473 nm, ϵ 1.5 × 10^4 M^{-1} cm^{-1}. ^{1}H NMR: δ 2.87 (m, 8H, PCH$_2$), 3.86 (m, 1H, =CH), 5.28 (s, 2H, CH_2Cl_2), 5.68 (d, J_{HH} = 5 Hz, 2H, H$_4$), 6.75 (d, J_{HH} = 5 Hz, 2H, H$_5$), 6.85−7.45 (42H, H$_{7,8}$ + Ph), 7.55 (d, J_{HH} = 8 Hz, 2H, H$_{10}$), 8.16 (d, J_{HH} = 8 Hz, 2H, H$_{11}$). ^{31}P NMR: δ 37.7 (s, PPh$_2$). SI MS: 1182 ([M − PF$_6$]$^+$, 75), 933 ([RuCl(dppe)$_2$]$^+$, 100), 897 ([Ru(dppe)$_2$ − H]$^+$, 70), 499 ([Ru(dppe) − H]$^+$, 100).

Synthesis of *trans*-[Ru{(*E*)-4,4′-C≡CC$_6$H$_4$CH=CHC$_6$H$_4$NO$_2$}Cl(dppe)$_2$] (33). A solution of *cis*-[RuCl$_2$(dppe)$_2$] (**10**; 200 mg, 0.21 mmol), (*E*)-4,4′-HC≡CC$_6$H$_4$CH=CHC$_6$H$_4$NO$_2$ (**4**; 80 mg, 0.32 mmol), and NaPF$_6$ (35 mg, 0.21 mmol) in CH_2Cl_2 (15 mL) was stirred for 3 h. Addition of petrol (50 mL) afforded a precipitate which was collected, dissolved in CH_2Cl_2 (15 mL), and stirred with NEt$_3$ (5 mL) for 1 h. The resultant mixture was passed through a basic alumina column, eluting with a 1:1 CH_2Cl_2/petrol mixture. The major orange band was collected and taken to dryness to afford **33** as an orange powder (200 mg, 72%). Recrystallization from CH_2Cl_2/heptane afforded orange crystals of the CH_2Cl_2 hemisolvate suitable for the X-ray diffraction study. Anal. Calcd for $C_{68}H_{58}ClNO_2P_4Ru\cdot0.5CH_2Cl_2$: C, 67.21; H, 4.86; N, 1.14. Found: C, 67.03; H, 4.74; N, 1.27. IR: ν(C≡C) 2064 m cm^{-1}. UV−vis: λ 490 nm, ϵ 2.6 × 10^4 M^{-1} cm^{-1}. ^{1}H NMR: δ 2.65 (m, 8H, PCH$_2$), 5.28 (s, 1H, CH_2Cl_2), 6.58 (d, J_{HH} = 4 Hz, 2H, H$_4$), 6.80−7.50 (44H, H$_{5,7,8}$ + Ph), 7.56 (d, J_{HH} = 4 Hz, 2H, H$_{10}$), 8.19 (d, J_{HH} = 4 Hz, 2H, H$_{11}$). ^{31}P NMR: δ 50.0. SI MS: 1181 ([M]$^+$, 100), 1146 ([M − Cl]$^+$, 20), 1100 ([M − Cl − NO$_2$]$^+$, 20), 897 ([Ru(dppe)$_2$ − H]$^+$, 20), 501 ([Ru(dppe) + H]$^+$, 65).

Crystal Structure Determinations of *trans*-[Ru(4-C≡CC$_6$H$_4$C≡CPh)Cl(dppm)$_2$] (15), *trans*-[Ru(4-C≡CC$_6$H$_4$CHO)Cl(dppe)$_2$] (29), and *trans*-[Ru{(*E*)-4,4′-C≡CC$_6$H$_4$CH=CHC$_6$H$_4$NO$_2$}Cl(dppe)$_2$] (33). Unique diffractometer data sets were obtained on Rigaku AFC6S (**29**) and AFC6R (**15**, **33**) diffractometers using the ω−2θ scan technique (graphite-monochromated Mo Kα radiation, 0.710 69 Å, 2θ_{max} = 55.2°, 296 K, **29**; graphite-monochromated Cu Kα radiation, 1.541 78 Å, 2θ_{max} = 120°, (**15**) (296 K), (**33**) (193 K)). An analytical absorption correction was applied for **15** and **29** and an empirical absorption correction for **33**. Data were corrected for Lorentz and polarization effects. Over the course of the data collection, the standards for **29** decreased by 1.2%; a linear correction factor was applied to the data to account for this. N independent reflections (N_o of these with $I \geq 2.00\sigma(I)$) were considered "observed" and used in full-matrix least-squares refinement. Anisotropic thermal parameters were refined for all non-hydrogen atoms in **15**, **29**, and **33**, except the disordered chlorine atoms of the solvent and lowered occupancy (see below) oxygen of the organometallic in **29** and the dichloromethane atoms in **33** (which refined to partial occupancy); (x, y, z, U_{iso})$_H$ were included constrained at estimated values. Conventional residuals R and R_w on $|F|$ are given; the weighting function $w = 1/\sigma^2(F_o) = [\sigma_c^2(F_o) + (p^2/4)F_o^2]^{-1}$ ($\sigma_c(F_o)$ = esd based on counting statistics, p = p factor determined experimentally from standard reflections) was employed. Computation used the teXsan package.[52] Specific data collection, solution and refinement parameters are given in Table 1. Pertinent results are given in the figures and tables.

Variations in Procedure for 29. The structure was solved by heavy-atom Patterson methods[35] and expanded using Fourier techniques.[36] The unit cell contains the $C_{61}H_{53}ClOP_4Ru$ species, a molecule of dichloromethane that is completely ordered, and a series of atomic sites approximately 3.0 Å apart running along the a axis, passing through the origin. The latter appear to be the chlorine atoms of disordered dichloromethane solvent molecules, Cl(4) and Cl(5) belonging to one molecule and Cl(6) and Cl(7) belonging to another. Restraints were initially placed on Cl···Cl intramolecular distances but were later removed, as doing so reduced the size of peaks in difference electron-density maps. The carbon (and hydrogen) atoms of the disordered dichloromethane molecules were not located. The oxygen atom of the $C_{61}H_{53}ClOP_4Ru$ molecule was observed to be disordered over two sites; the relative populations have been refined. Several reflections, especially those of the type 00l, showed evidence of overlap and/or diffuse scattering and were omitted.

HRS Measurements. An injection seeded Nd:YAG laser (Q-switched Nd:YAG Quanta Ray GCR, 1064 nm, 8 ns pulses, 10 Hz) was focused into a cylindrical cell (7 mL) containing the sample. The intensity of the incident beam was varied by rotation of a half-wave plate placed between crossed polarizers. Part of the laser pulse was sampled by a photodiode to measure the vertically polarized incident light intensity. The frequency-doubled light was collected by an efficient condenser system and detected by a photomultiplier. The harmonic scattering and linear scattering were distinguished by appropriate filters; gated integrators were used to obtain intensi-

(35) Beurskens, P. T.; Admiraal, G.; Bosman, W. P.; Garcia-Granda, S.; Gould, R. O.; Smits, J. M. M.; Smykalla, C. PATTY; Technical Report of the Crystallographic Laboratory; University of Nijmegen, Nijmegen, The Netherlands, 1992.

(36) Beurskens, P. T.; Admiraal, G.; Bosman, W. P.; Garcia-Granda, S.; Gould, R. O.; Smits, J. M. M.; Smykalla, C. The DIRDIF-94 Program System; Technical Report of the Crystallographic Laboratory; University of Nijmegen, Nijmegen, The Netherlands, 1994.

Scheme 1. Synthesis of (*E*)-4,4′-HC≡CC_6H_4CH=$CHC_6H_4NO_2$ (4)[a]

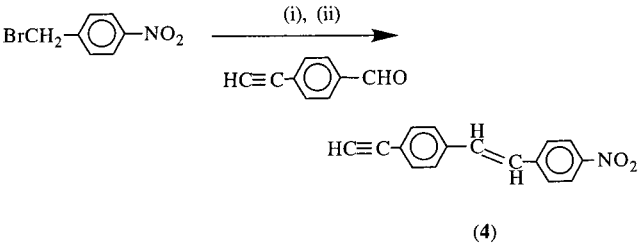

(4)

[a] Legend: (i) $P(OEt)_3$, Δ; (ii) NaOMe.

Scheme 2. Synthesis of 4,4′,4″-HC≡CC_6H_4C≡CC_6H_4C≡$CC_6H_4NO_2$ (6)[a]

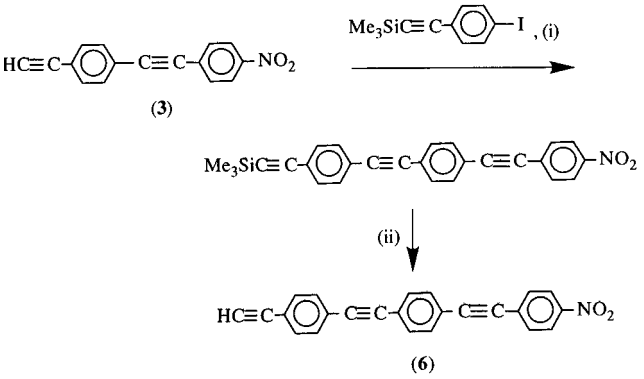

(6)

[a] Legend: (i) $PdCl_2(PPh_3)_2$, CuI; (ii) NBu_4F.

ties of the incident and harmonic scattered light. All measurements were performed in thf using *p*-nitroaniline ($\beta = 21.4 \times 10^{-30}$ esu[37]) as a reference.

Z-Scan Measurements. Measurements were performed at 800 nm using a system consisting of a Coherent Mira Ti−sapphire laser generating a mode-locked train of approximately 100 fs pulses and a home-built Ti−sapphire regenerative amplifier pumped with a frequency-doubled Q-switched pulsed YAG laser (Spectra Physics GCR) at 30 Hz and employing chirped pulse amplification.

thf solutions were examined in a glass cell with a 0.1 cm path length. The Z-scans were recorded at two concentrations for each compound and the real and imaginary parts of the nonlinear phase shift determined by numerical fitting.[38] The real and imaginary parts of the hyperpolarizability of the solute were then calculated by assuming linear concentration dependencies of the solution susceptibility. The nonlinearities and light intensities were calibrated using measurements of a 1 mm thick silica plate, for which the nonlinear refractive index $n_2 = 3 \times 10^{-16}$ cm^2 W^{-1} was assumed.

Results and Discussion

Synthesis and Characterization of Vinylidene and Alkynyl Complexes. New acetylenes required for the vinylidene and alkynyl complex syntheses were prepared by established organic synthetic procedures (Schemes 1 and 2). We have previously reported the synthesis of (*E*)-4,4′-HC≡CC_6H_4CH=$CHC_6H_4NO_2$ (**4**)[7,34] using the standard Wittig method; the *E* isomer can be separated from the *Z* isomer by fractional crystallization. Our interest in these earlier studies was, inter alia, in comparing the optical nonlinearities of alkynyl complexes containing either *Z*- or *E*-configured ligands.[12−14] For the current studies, a higher yielding synthesis of the more efficient *E* isomer was required; therefore, Emmons−Horner−Wadsworth protocols were employed, affording **4** in 85% yield. Dixneuf has reported that coupling 4-iodo((trimethylsilyl)ethynyl)benzene to 4-ethynylnitrobenzene, followed by deprotection with base, affords 4,4′-HC≡CC_6H_4C≡$CC_6H_4NO_2$ (**3**) in good yield.[23] We have now found that this process can be repeated to couple 4-iodo((trimethylsilyl)ethynyl)benzene with **3**, affording 4,4′,4″-Me_3SiC≡CC_6H_4C≡CC_6H_4C≡$CC_6H_4NO_2$ (**5**), subsequent deprotection with base affording 4,4′,4″-HC≡CC_6H_4C≡CC_6H_4C≡$CC_6H_4NO_2$ (**6**). The new acetylenes were characterized by IR, UV−vis, and ^{1}H NMR spectroscopy and mass spectrometry.

The synthetic methodology employed for the preparation of the new vinylidene and alkynyl complexes (Scheme 3) has been successfully utilized for the preparation of **12**, **26**, **27**, **30**, and **31** by Dixneuf and co-workers,[30,33] for **13**, **19**, and **25** by us,[31] and for **18** by Lewis and co-workers.[32] Complexes **14**−**17**, **20**−**25**, **28**, **29**, **32**, and **33** were characterized by IR and ^{1}H and ^{31}P NMR spectroscopy and secondary ion mass spectrometry. IR spectra of the alkynyl complexes contain characteristic ν(C≡C) bands at around 2060 cm^{-1} for the metal-bound alkynyl group, whereas those of the vinylidene complexes contain strong ν(PF) bands at around 840 cm^{-1} corresponding to the PF_6^- counterion. The ^{1}H NMR spectra of the vinylidene complexes contain characteristic multiplets at 3.05−3.17 ppm for the protons attached to the β-carbon of the metal-bound vinylidene unit of the dppm-containing complexes, resonances which move to lower field for the dppe-containing examples. The ^{31}P NMR spectra contain one singlet resonance, confirming the trans-disposed arrangement of the diphosphine ligands; the phosphorus signals for the vinylidene complexes are uniformally 10−15 ppm upfield of resonances in the corresponding alkynyl complexes. The mass spectra contain molecular ions (alkynyl complexes) or cationic ions (vinylidene complexes), with fragment ions corresponding to loss of chlorine and alkynyl/vinylidene ligands.

X-ray Structural Studies of *trans*-[Ru(4,4′−C≡CC_6H_4C≡CPh)Cl(dppm)$_2$] (15), *trans*-[Ru(4-C≡CC_6H_4CHO)Cl(dppe)$_2$] (29), and *trans*-[Ru{(*E*)-4,4′−C≡CC_6H_4CH=$CHC_6H_4NO_2$}Cl(dppe)$_2$] (33). We have confirmed the composition of complexes **15**, **29**, and **33** by single-crystal X-ray diffraction studies. Crystal data are collected in Table 1, and important bond lengths and angles are displayed in Table 2. ORTEP plots of **15**, **29**, and **33** are displayed in Figures 2−4, respectively. Most bond lengths and angles about the Cl−Ru−C(1)−C(2)−C(3) units in these structures are not unusual. The Cl−Ru, Ru−C(1), and C(2)−C(3) data for all complexes fall within the range of those previously reported for related octahedral *trans*-bis(bidentate phosphine)ruthenium alkynyl complexes.[31,32,39−42] The C(1)−C(2) bond length for **29** is surprisingly short (1.158(5) Å), the only other such short C(1)−C(2) vector being that of the ethynyl complex

(37) Stähelin, M.; Burland, D. M.; Rice, J. E. *Chem. Phys. Lett.* **1992**, *191*, 245.

(38) Sheik-Bahae, M.; Said, A. A.; Wei, T.; Hagan, D. J.; van Stryland, E. W. *IEEE J. Quantum Electron.* **1990**, *26*, 760.

(39) Haquette, P.; Pirio, N.; Touchard, D.; Toupet, L.; Dixneuf, P. H. *J. Chem. Soc., Chem. Commun.* **1993**, 163.

(40) Faulkner, C. W.; Ingham, S. L.; Khan, M. S.; Lewis, J.; Long, N. J.; Raithby, P. R. *J. Organomet. Chem.* **1994**, *482*, 139.

(41) Naulty, R. H.; McDonagh, A. M.; Whittall, I. R.; Cifuentes, M. P.; Humphrey, M. G.; Houbrechts, S.; Maes, J.; Persoons, A.; Heath, G. A.; Hockless, D. C. R. *J. Organomet. Chem.* **1998**, *563*, 137.

Scheme 3. Synthetic Procedure for the Preparation of Vinylidene and Alkynyl Complexes 12−33

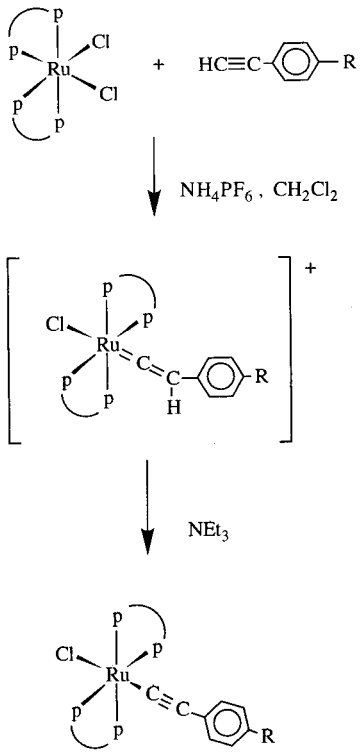

p p	R	Vinylidene Complex	Ref.
dppm	H	**12**	33
	C≡CPh	**14**	This work
	CHO	**16**	This work
	NO_2	**18**	32
	4-C≡C$C_6H_4NO_2$	**20**	This work
	4,4'-C≡CC_6H_4C≡C$C_6H_4NO_2$	**22**	This work
	(*E*)- 4-CH=CH$C_6H_4NO_2$	**24**	This work
dppe	H	**26**	33

p p	R	Acetylide Complex	Ref.
dppm	H	**13**	31
	C≡CPh	**15**	This work
	CHO	**17**	This work
	NO_2	**19**	31
	4-C≡C$C_6H_4NO_2$	**21**	This work
	4,4'-C≡CC_6H_4C≡C$C_6H_4NO_2$	**23**	This work
	(*E*)- 4-CH=CH$C_6H_4NO_2$	**25**	31
dppe	H	**27**	33
	CHO	**29**	This work
	NO_2	**31**	33
	(*E*)- 4-CH=CH$C_6H_4NO_2$	**33**	This work

Table 2. Important Structural Parameters (Distances in Å, Angles in deg) for 15, 29, and 33

	15	**28**	**33**
Ru−Cl	2.482(2)	2.507(1)	2.489(1)
Ru−C(1)	1.984(8)	2.012(4)	1.996(4)
C(1)−C(2)	1.20(1)	1.158(5)	1.205(7)
C(2)−C(3)	1.43(1)	1.457(6)	1.434(7)
C(9)−C(10)	1.18(1)		1.304(9)
Cl−Ru−C(1)	175.9(2)	179.1(1)	171.8(1)
Ru−C(1)−C(2)	178.7(8)	176.5(4)	177.4(4)
C(1)−C(2)−C(3)	178(1)	178.2(5)	174.4(5)

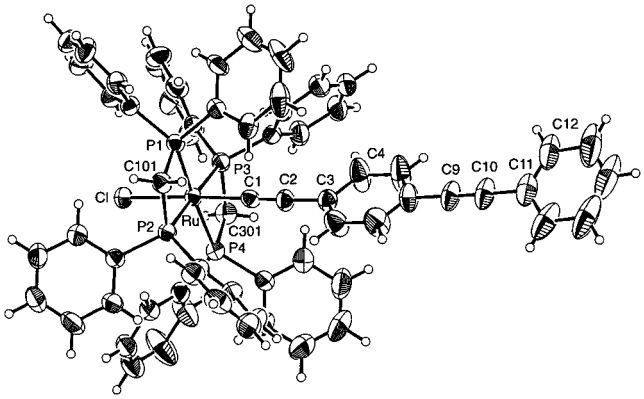

Figure 2. Molecular geometry and atomic labeling scheme for *trans*-[Ru(4-C≡CC_6H_4C≡CPh)Cl(dppm)$_2$] (**15**). Thermal ellipsoids at the 20% probability level are shown for the non-hydrogen atoms.

trans-[Ru(C≡CH)Cl(dppm)$_2$] (1.162(9) Å).[30,39] Of particular interest for NLO merit is the coplanarity of phenyl rings in the alkynyl ligand; we have previously used semiempirical ZINDO to examine the effect upon

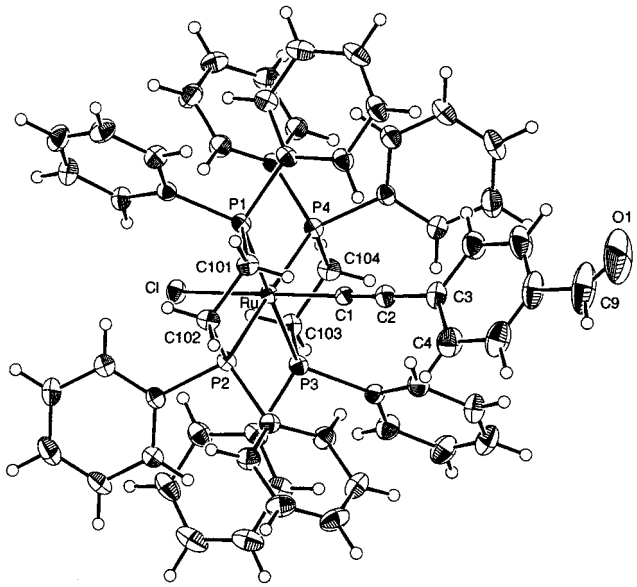

Figure 3. Molecular geometry and atomic labeling scheme for *trans*-[Ru(4-C≡CC_6H_4CHO)Cl(dppe)$_2$] (**29**). Thermal ellipsoids at the 20% probability level are shown for the non-hydrogen atoms.

quadratic optical nonlinearity of phenyl−phenyl rotation in *trans*-[Ru(4,4′-C≡C$C_6H_4C_6H_4NO_2$)Cl(dppm)$_2$], for which a variation of 50% was found between maximum (coplanarity) and minimum (orthogonality) responses.[31] Coplanarity, along with efficient delocalization, is therefore important for maximizing NLO response in the present complexes. The phenyl−phenyl dihedral angles for the 4-(phenylethynyl)phenylethynyl ligand in **15** (26.75°) and the 4-nitro-(*E*)-stilbenylalkynyl ligand in **33** (59.27°) are significantly distorted from the idealized coplanarity (0°). No structural studies of complexes with the alkynyl ligand from **15** have been reported previ-

(42) Younus, M.; Long, N. J.; Raithby, P. R.; Lewis, J.; Page, N. A.; White, A. J. P.; Williams, D. J.; Colbert, M. C. B.; Hodge, A. J.; Khan, M. S.; Parker, D. G. *J. Organomet. Chem.* **1999**, *578*, 198.

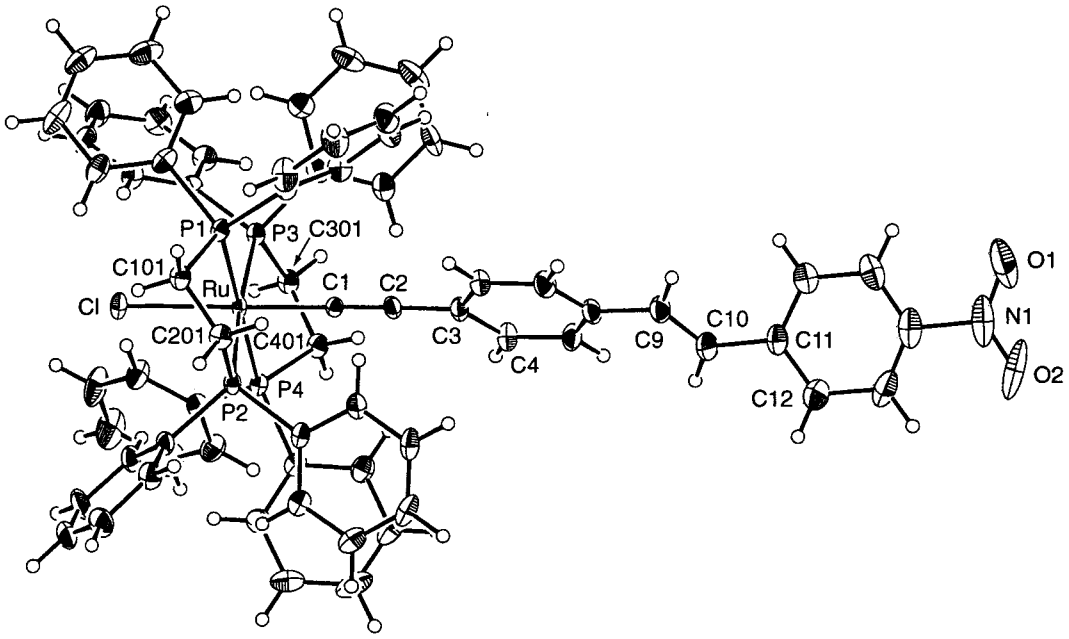

Figure 4. Molecular geometry and atomic labeling scheme for *trans*-[Ru{(*E*)-4,4′-C≡CC_6H_4CH═$CHC_6H_4NO_2$}Cl(dppe)$_2$] (**33**). Thermal ellipsoids at the 20% probability level are shown for the non-hydrogen atoms.

ously. However, all previous structural reports of complexes with the 4-nitro-(*E*)-stilbenylalkynyl ligand reveal a deviation from coplanarity, viz. Ru{(*E*)-4,4′-C≡CC_6H_4CH═$CHC_6H_4NO_2$}$(PPh_3)_2(\eta$-$C_5H_5)$ (18.80°),[7] Ni{(*E*)-4,4′-C≡CC_6H_4CH═$CHC_6H_4NO_2$}$(PPh_3)(\eta$-$C_5H_5)$ (42.35°),[43] and Au{(*E*)-4,4′-C≡CC_6H_4CH═CHC_6H_4-NO_2}(PPh_3) (5.53°).[44] Such deviations from coplanarity are likely due to a combination of vinyl H−ortho H repulsion and packing forces.

Electrochemical Studies. Alkynyl complexes are potentially useful as electronic or optoelectronic materials, and their electrochemical properties are an important indicator in this regard; the electrochemistry of alkynylmetal complexes is therefore a subject of significant current interest. Of specific relevance to the present studies, a number of reports have considered the electrochemical properties of *trans*-bis(bidentate phosphine)ruthenium alkynyl complexes,[41,42,45−48] but, with the exception of our brief earlier report,[41] the focus of these studies has been on bis(alkynyl) complexes. The results of cyclic voltammetric investigations of complexes **8**−**33** are summarized in Table 3.

Anodic Behavior. All of the complexes studied display an anodic wave assigned to the $Ru^{II/III}$ oxidation process. The first oxidation process in the alkynyl complexes occurs with potentials ranging from 0.54 to 0.74 V, the higher potentials being characteristic of complexes with a single-phenyl-ring arylalkynyl ligand containing the electron-withdrawing substituent NO_2 or CHO. In each case this process is either reversible or quasi-reversible (ΔE = 0.06−0.08 V, $i_{pc}/i_{pa} \sim 1$, employing standard conditions of 100 mV s^{-1} scan rate at room temperature). As expected, a sizable shift toward more positive potentials is observed for the oxidation process in the positively charged vinylidene complexes, with the $Ru^{II/III}$ oxidation found at potentials in the range of 1.23−1.57 V; again, the higher potentials are observed for complexes containing electron-withdrawing aryl substituents. In contrast to the alkynyl complexes, the $Ru^{II/III}$ couple in the vinylidene complexes is irreversible under our standard conditions, approaching quasi-reversible behavior on increasing the scan rate. For example, Figure 5 shows the oxidative cyclic voltammetric behavior for the vinylidene complex [Ru(C═CHPh)Cl$(dppm)_2$]PF_6 (**12**) using scan rates ranging from 100 to 1200 mV s^{-1}. The $Ru^{II/III}$ oxidation has been labeled A (ΔE = 0.19 V). The signal labeled B is associated with the main $Ru^{II/III}$ oxidation process and displays a signal current independent of the scan rate; it is attributed to a redox process involving the [Ru(C═CHPh)Cl$(dppm)_2]^{2+}$ daughter product of the $Ru^{II/III}$ oxidation process. Higher scan rates reveal a cathodic peak (labeled C) at a potential similar to that observed for the corresponding alkynyl complex, suggesting conversion of the [Ru(C═CHPh)Cl$(dppm)_2]^{2+}$ product to the corresponding alkynyl cation by loss of a proton and subsequent reduction to the neutral alkynyl complex (Scheme 4). A similar deprotonation of an oxidized vinylidene complex to afford an alkynyl complex has been noted previously.[53]

In some cases a second, less reversible, anodic process is observed at higher potentials, ranging from 1.42 to

(43) Whittall, I. R.; Humphrey, M. G.; Hockless, D. C. R. *Aust. J. Chem.* **1998**, *51*, 219.
(44) Whittall, I. R.; Humphrey, M. G.; Hockless, D. C. R. *Aust. J. Chem.* **1997**, *50*, 991.
(45) Colbert, M. C. B.; Lewis, J.; Long, N. J.; Raithby, P. R.; White, A. J. P.; Williams, D. J. *J. Chem. Soc., Dalton Trans.* **1997**, 99.
(46) Jones, N. D.; Wolf, M. O. *Organometallics* **1997**, *16*, 1352.
(47) Lebreton, C.; Touchard, D.; Le Pichon, L.; Daridor, A.; Toupet, L.; Dixneuf, P. H. *Inorg, Chim. Acta* **1998**, *272*, 188.
(48) Choi, M.-Y.; Chan, M. C.-W.; Zhang, S.; Cheung, K.-K.; Che, C.-M.; Wong, K.-Y. *Organometallics* **1999**, *18*, 2074.
(49) Cheng, L.-T.; Tam, W.; Stevenson, S. H.; Meredith, G. R.; Rikken, G.; Marder, S. R. *J. Phys. Chem.* **1991**, *95*, 10631.
(50) Kanis, D. R.; Ratner, M. A.; Marks, T. J. *Chem. Rev.* **1994**, *94*, 195.
(51) Bhawalkar, J. D.; He, G. S.; Prasad, P. N. *Rep. Prog. Phys.* **1996**, *59*, 1041.
(52) teXsan: Single-Crystal Structure Analysis Software, Version 1.8; Molecular Structure Corp., The Woodlands, TX, 1997.
(53) Bianchini, C.; Meli, A.; Perluzzi, M.; Zanobini, F.; Zanello, P. *Organometallics* **1990**, *9*, 241.

Table 3. Cyclic Voltammetric Data for Complexes 8−21 and 23−33[a]

complex	$E°_{ox}$ (V) [i_{pc}/i_{pa}] $Ru^{II/III}$	$E°_{red}$ (V) [i_{pa}/i_{pc}] $A^{0/-I}$
cis-[$RuCl_2(dppm)_2$] (**8**)	0.99 [0.9]	
trans-[$RuCl_2(dppm)_2$] (**9**)[b]	0.62 [1]	
cis-[$RuCl_2(dppe)_2$] (**10**)	0.96 [0.9]	
trans-[$RuCl_2(dppe)_2$] (**11**)	0.65 [1]	
trans-[Ru(C═CHPh)Cl$(dppm)_2$]PF_6 (**12**)	1.38[c]	−1.15[d]
trans-[Ru(C≡CPh)Cl$(dppm)_2$] (**13**)	0.55 [1]	
trans-[Ru(4-C═CHC_6H_4C≡CPh)Cl$(dppm)_2$]PF_6 (**14**)	1.34[c]	−1.11[d]
trans-[Ru(4-C≡CC_6H_4C≡CPh)Cl$(dppm)_2$] (**15**)	0.55 [0.9]	
trans- [Ru(4-C═CHC_6H_4CHO)Cl$(dppm)_2$]PF_6 (**16**)	1.50[c]	−1.18[d]
trans-[Ru(4-C≡CC_6H_4CHO)Cl$(dppm)_2$] (**17**)	0.66 [1]	
trans-[Ru(4-C═$CHC_6H_4NO_2$)Cl$(dppm)_2$]PF_6 (**18**)	1.56[c]	−0.82 [0.9], −1.12[d]
trans-[Ru(4-C≡$CC_6H_4NO_2$)Cl$(dppm)_2$] (**19**)	0.72 [1]	−0.81 [0.7], −1.08[d]
trans-[Ru(4,4′-C═CHC_6H_4C≡$CC_6H_4NO_2$)Cl$(dppm)_2$]PF_6 (**20**)	1.42[c]	−0.83 [0.9]
trans-[Ru(4,4′-C≡CC_6H_4C≡$CC_6H_4NO_2$)Cl$(dppm)_2$] (**21**)	0.57 [0.9]	−0.90 [0.7]
trans-[Ru(4,4′,4″-C≡CC_6H_4C≡CC_6H_4C≡$CC_6H_4NO_2$)Cl$(dppm)_2$] (**23**)	0.54 [1]	−0.86 [0.9]
trans-[Ru{(*E*)-4-C═CHC_6H_4CH═CH-4-$C_6H_4NO_2$}Cl$(dppm)_2$]PF_6 (**24**)	1.24[c]	−0.84[d]; −1.01 [0.8]
trans-[Ru{(*E*)-4-C≡CC_6H_4CH═CH-4-$C_6H_4NO_2$}Cl$(dppm)_2$] (**25**)[c]	0.56 [1]	−0.87 [0.4]
trans-[Ru(C═CHPh)Cl$(dppe)_2$]PF_6 (**26**)	1.36[c]	−1.13[d]
trans-[Ru(C≡CPh)Cl$(dppe)_2$] (**27**)	0.55 [1]	
trans- [Ru(4-C═CHC_6H_4CHO)Cl$(dppe)_2$[PF_6 (**28**)	1.48[c]	−1.15[d]
trans-[Ru(4-C≡CC_6H_4CHO)Cl$(dppe)_2$] (**29**)	0.68 [1]	
trans-[Ru(4-C═$CHC_6H_4NO_2$)Cl$(dppe)_2$]PF_6 (**30**)	1.57[c]	−0.83;[b] −1.10 [0.8]
trans-[Ru(4-C≡$CC_6H_4NO_2$)Cl$(dppe)_2$] (**31**)	0.74 [0.9]	−0.84 [0.8]; −1.10 [0.9]
trans-[Ru{(*E*)-4,4′-C═CHC_6H_4CH═$CHC_6H_4NO_2$}Cl$(dppe)_2$]PF_6 (**32**)	1.23[c]	−0.79 [0.9]; −1.0[d]
trans-[Ru{(*E*)-4,4′-C≡CC_6H_4CH═$CHC_6H_4NO_2$}Cl$(dppe)_2$] (**33**)	0.55 [1]	−0.98 [1]

[a] Conditions: CH_2Cl_2; Pt-wire auxiliary, Pt working, and Ag/AgCl reference electrodes; ferrocene/ferrocenium couple located at 0.56 V. [b] Reference 41. [c] $E_{pa}(Ru^{II/III})$ (V) for nonreversible process. [d] $E_{pc}(A^{0/-1})$ (V) for nonreversible process.

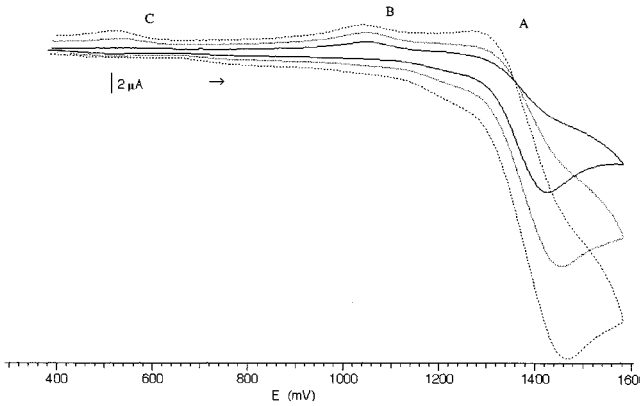

Figure 5. Effect of varying the scan rate from 100 (dashed line) through 400 to 1200 mV s^{-1} (solid line) on the oxidative behavior of [Ru(C═CHPh)Cl$(dppm)_2$]PF_6 (**12**).

Scheme 4. Proposed Anodic Behavior for the Vinylidene Complex *trans*-[Ru(C═CHPh)Cl$(dppm)_2$]PF_6 (12)

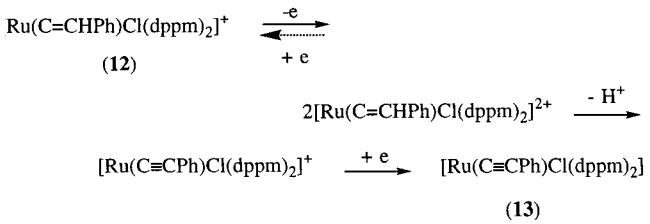

1.57 V, attributed to the $Ru^{III/IV}$ oxidation process. The highest potential recorded for this second oxidation is, not surprisingly, that of the 4-nitrophenylvinylidene complex *trans*-[Ru(4-C═$CHC_6H_4NO_2$)Cl$(dppe)_2$]PF_6 (**30**).

Examination of the cyclic voltammetric data for these alkynyl and vinylidene complexes affords a series of trends.

(i) The familiar increase in the $Ru^{II/III}$ oxidation potential on addition of the electron-withdrawing nitro group to the arylalkynyl ligand[9] was observed for all of the relevant complexes in this study, with similar increases found for both the alkynyl and vinylidene groups: e.g., increases of 0.17 and 0.18 V were found on proceeding from *trans*-[Ru(C≡CPh)Cl$(dppm)_2$] (**13**; 0.55 V) to *trans*-[Ru(4-C≡$CC_6H_4NO_2$)Cl$(dppm)_2$] (**19**; 0.72 V) and from *trans*-[Ru(C═CHPh)Cl$(dppm)_2$]PF_6 (**12**; 1.38 V) to *trans*-[Ru(4-C═$CHC_6H_4NO_2$)Cl$(dppm)_2$]-PF_6 (**18**; 1.56 V), respectively.

(ii) A similar trend was observed on addition of an aldehyde moiety, with oxidation potentials being only slightly lower than those of the analogous nitro-containing complexes: e.g., the $Ru^{II/III}$ oxidation potential for *trans*-[Ru(4-C≡$CC_6H_4NO_2$)Cl$(dppm)_2$] (**19**) was found at 0.72 V, compared to 0.68 V for *trans*-[Ru(4-C≡CC_6H_4-CHO)Cl$(dppm)_2$] (**17**), and the vinylidene complexes showed a similar trend, viz. *trans*-[Ru(4-C═CHC_6H_4-NO_2)Cl$(dppm)_2$]PF_6 (**18**; 1.56 V) and *trans*-[Ru(4-C═CHC_6H_4CHO)Cl$(dppm)_2$]PF_6 (**16**; 1.50 V).

(iii) Replacement of the dppm coligand with dppe was found to have little effect on oxidation potentials, as expected from the similar electron-donating properties of the diphosphines.

(iv) Chain lengthening of the nitro-containing vinylidene ligand was found to produce a decrease in the $Ru^{II/III}$ oxidation potential: e.g., from 1.56 V for *trans*-[Ru(4-C═$CHC_6H_4NO_2$)Cl$(dppm)_2$]PF_6 (**18**) to 1.42 V for *trans*-[Ru(4,4′-C═CHC_6H_4C≡$CC_6H_4NO_2$)Cl$(dppm)_2$]-PF_6 (**20**). We have previously noted a similar decrease in the oxidation potential required for the $Ru^{II/III}$ process on chain lengthening of alkynyl complexes.[9] This effect is attenuated on further chain lengthening, e.g. in proceeding from *trans*-[Ru(4-C≡$CC_6H_4NO_2$)Cl$(dppm)_2$] (**19**; 0.72 V) to *trans*-[Ru(4,4′-C≡CC_6H_4C≡$CC_6H_4NO_2$)-Cl$(dppm)_2$] (**21**; 0.57 V) and then to *trans*-[Ru(4,4′,4″-C≡CC_6H_4C≡CC_6H_4C≡$CC_6H_4NO_2$)Cl$(dppm)_2$] (**23**; 0.54 V), with the last compound possessing an $E°_{ox}$ value similar to that of *trans*-[Ru(C≡CPh)Cl$(dppm)_2$] (**13**; 0.55

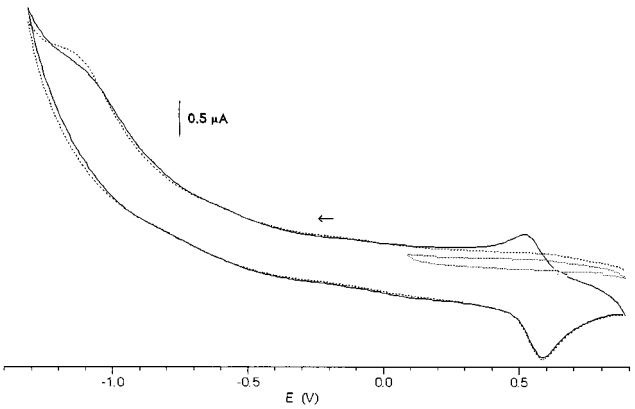

Figure 6. Comparison of results from cathodic cyclic voltammetric scans for [Ru(4,4′-C═CHC$_6$H$_4$C≡CPh)Cl(dppm)$_2$]PF$_6$ (**14**) using switching potentials of −1.4 (two successive scans) and 0 V.

V), which lacks an acceptor group. In the present study, the absence of an acceptor group influencing the oxidation potential results in chain lengthening from the phenylalkynyl complex **13** to *trans*-[Ru(4,4′-C≡CC$_6$H$_4$C≡CPh)Cl(dppm)$_2$] (**15**) having no effect on the oxidation potentials (both 0.55 V); the corresponding vinylidene complexes were also found to have similar oxidation potentials (1.38 V, **12**; 1.34 V, **14**).

Cathodic Behavior. Cyclic voltammetric scans to −1.4 V were carried out for each complex; results are summarized in Table 3 and were found to be dependent on the length and substituents of the alkynyl ligand, as well as on the charge of the complex. The following may be noted.

(i) Alkynyl complexes **13**, **15**, and **27** (which lack a formal acceptor substituent) and complexes **17** and **29** (containing the aldehyde group) displayed no reduction peaks in the region sampled.

(ii) Vinylidene complexes **12**, **14**, and **26** (lacking formal acceptor groups) showed a single, nonreversible reduction process occurring with potentials in the range −1.11 to −1.15 V; similarly, the vinylidene complexes **16** and **28** (containing aldehyde substituents) showed a single process at slightly more negative potentials (−1.15 to −1.18 V), presumably due to the metal-centered Ru$^{I/II}$ reduction. Varying the scan rate from 100 to 1000 mV s^{-1} was found to have little effect on the reversibility of this redox process.

(iii) The (4-nitrophenyl)alkynyl complexes (**19** and **31**) and corresponding vinylidene complexes (**18** and **30**) displayed two reduction processes, typically centered at potentials of −0.8 and −1.1 V, presumably due to the Ru$^{I/II}$ and NO$_2$ reduction processes. The 4-nitro-(*E*)-stilbenylvinylidene complexes **24** and **32** displayed cathodic scans very similar to those of the (4-nitrophenyl)vinylidene complexes. In contrast, the 4-nitro-(*E*)-stilbenylalkynyl complexes **25** and **33**, and complexes **20** and **21**, showed only a single reduction process at around −1.0 V.

(iv) Figure 6 shows the cathodic behavior for *trans*-[Ru(4-C═CHC$_6$H$_4$C≡CPh)Cl(dppm)$_2$]PF$_6$ (**14**), using a starting potential of 0.8 V and a switching potential just beyond that required for the first vinylidene reduction process, in this case −1.4 V. Initial scans and scans using a switching potential of 0 V (dotted lines) show no oxidation peaks around 0.5 V. When the scan is extended past the vinylidene complex reduction process, however, a reversible oxidation process is apparent at 0.5 V, suggesting conversion of the reduced vinylidene complex to the corresponding alkynyl complex via hydrogen loss (Scheme 5). Similar reduction of the vinylidene complex to the alkynyl complex with loss of hydrogen has been noted previously.[53]

Scheme 5. Proposed Cathodic Behavior for the Vinylidene Complex *trans*-[Ru(4-C═CHC$_6$H$_4$C≡CPh)Cl(dppm)$_2$]PF$_6$ (14)

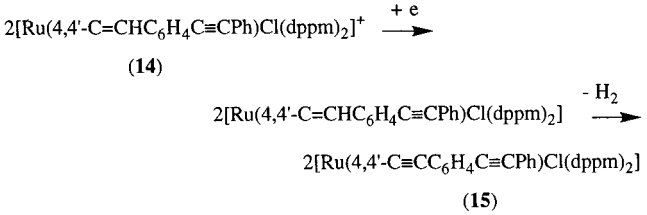

Linear Optical Spectroscopy. Absorption maxima and intensities from electronic spectra are collected in Table 4. We have previously shown that these low-energy transitions can be assigned as MLCT bands.[41] The two-level model suggests that the energy and oscillator strength of these charge-transfer bands are important determinants of NLO merit. Gauging the effects of structural modification on λ_{max} and ϵ are therefore potentially important as predictors of quadratic, and possibly cubic, optical nonlinearity, and a comparison with the effects of these modifications on quadratic nonlinearity provides a test for the two-level model. Examining the tabulated data, a number of trends are apparent.

(i) Introduction of an acceptor group in proceeding from 4-H to 4-CHO and 4-NO$_2$ aryl-substituted complexes results in a dramatic red shift in λ_{max}, with λ_{max} of the nitro-containing complexes at lowest energy.

(ii) A small red shift in λ_{max} is seen in most instances in proceeding from dppm- to dppe-containing complexes.

(iii) Proceeding from the vinylidene complex to the analogous alkynyl complex results in little change in λ_{max} (a small red shift usually being observed), but an increase in ϵ is observed in most cases.

(iv) Chain lengthening in proceeding from **12** and **13** to **14** and **15** results in a significant red shift in λ_{max}, a result of extending the π-system; in contrast, chain lengthening in the dipolar NO$_2$-containing complexes in proceeding from **19** to **21** to **23** results in a blue shift in λ_{max}, as the acceptor substituent becomes increasingly remote from the donor ligated-ruthenium atom.

(v) Replacing the yne by an ene linkage in proceeding from **20** and **21** to **24** and **25** results in a significant red shift in λ_{max}.

Quadratic Hyperpolarizabilities. We have determined the molecular quadratic nonlinearities of complexes **12**−**21** and **23**−**33**, together with those of some precursor acetylenes, using hyper-Rayleigh scattering at 1064 nm; the results of these studies, β_{exp}, are given in Table 4, together with the two-level-corrected values, β_0. The two-state model may not be adequate for the donor−acceptor organometallic complexes in this study. It has been suggested that the two-state model is appropriate in the limited cases where structural change is restricted to the molecular component responsible for the charge-transfer band contributing to the hyperpo-

Table 4. Experimental Linear and Nonlinear Optical Response Parameters[a]

complex	λ_{max} (nm) (ϵ, 10^4 M^{-1} cm^{-1})	β_{exp} (10^{-30} esu)	β_0 (10^{-30} esu)	γ_{real} (10^{-36} esu)	γ_{imag} (10^{-36} esu)	$\lvert\gamma\rvert$ (10^{-36} esu)
4-HC≡CC_6H_4C≡CPh (**1**)	316 (2.9)	*i*	*i*	25 ± 10	<6	25 ± 10
4-HC≡$CC_6H_4NO_2$ (**2**)	288 (2.8)[d]	14[d]	9	<80	10 ± 5	10 ± 5
4,4′-HC≡CC_6H_4C≡$CC_6H_4NO_2$ (**3**)	331 (2.8)[d]	31[d]	17	120 ± 20	0	120 ± 20
(*E*)−4,4′-HC≡CC_6H_4CH═$CHC_6H_4NO_2$ (**4**)	358 (3.3)[d]	55[d]	27	*i*	*i*	*i*
4-HC≡CC_6H_4CHO (**7**)	271 (2.5)	7	4	17 ± 8	0	17 ± 8
trans-[Ru(C═CHPh)Cl(dppm)$_2$]PF_6 (**12**)	320 (sh) (0.6)	24	16	<440	<50	<440
trans-[Ru(C≡CPh)Cl(dppm)$_2$] (**13**)	308 (1.7)[e]	20[e]	12	<120	0	<120
trans-[Ru(4-C═CHC_6H_4C≡CPh)Cl(dppm)$_2$]PF_6 (**14**)	380 (2.1)	64	31	<500	0	<500
trans-[Ru(4-C≡CC_6H_4C≡CPh)Cl(dppm)$_2$] (**15**)	381 (2.9)	101	43	65 ± 40	520 ± 200	520 ± 200
trans-[Ru(4-C═CHC_6H_4CHO)Cl(dppm)$_2$]PF_6 (**16**)	403 (1.9)	108	39	0	<20	<20
trans-[Ru(4-C≡CC_6H_4CHO)Cl(dppm)$_2$] (**17**)	405 (6.0)	106	38	<120	210 ± 60	210 ± 60
trans-[Ru(4-C═$CHC_6H_4NO_2$)Cl(dppm)$_2$]PF_6 (**18**)	470 (1.1)	721	127	<50	<30	<50
trans-[Ru(4-C≡$CC_6H_4NO_2$)Cl(dppm)$_2$] (**19**)	473 (1.8)[e]	767[e]	129	170 ± 34[c,f]	230 ± 46[c,f]	290 ± 60
trans-[Ru(4,4′-C═CHC_6H_4C≡$CC_6H_4NO_2$)Cl(dppm)$_2$]PF_6 (**20**)	326 (2.2)[h]	424	122	<500	420 ± 60	420 ± 60
trans-[Ru(4,4′-C≡CC_6H_4C≡$CC_6H_4NO_2$)Cl(dppm)$_2$] (**21**)	464 (1.4)	833	161	−160 ± 80	160 ± 60	230 ± 100
trans-[Ru(4,4′,4″-C≡CC_6H_4C≡CC_6H_4C≡$CC_6H_4NO_2$)Cl(dppm)$_2$] (**23**)	439 (2.0)	1379	365	−920 ± 200	970 ± 200	1300 ± 300
trans-[Ru{(*E*)-4,4′-C═CHC_6H_4CH═$CHC_6H_4NO_2$}Cl(dppm)$_2$]PF_6 (**24**)	369 (1.9)[h]	1899	314	*b*	*b*	*b*
trans-[Ru{(*E*)-4,4′-C≡CC_6H_4CH═$CHC_6H_4NO_2$}Cl(dppm)$_2$] (**25**)	490 (2.6)[e]	1964[e]	235	200 ± 40[c,f]	1100 ± 220[c,f]	1100 ± 220
trans-[Ru(C═CHPh)Cl(dppe)$_2$]PF_6 (**26**)	317 (1.5)	*b*		380 ± 400	<50	380 ± 400
trans-[Ru(C≡CPh)Cl(dppe)$_2$] (**27**)	319 (1.8)	6	3	−170 ± 40[c,g]	71 ± 20[c,g]	180 ± 45
trans-[Ru(4-C═CHC_6H_4CHO)Cl(dppe)$_2$]PF_6 (**28**)	412 (2.0)	181	61	<260	0	<260
trans-[Ru(4-C≡CC_6H_4CHO)Cl(dppe)$_2$] (**29**)	413 (2.8)	120	40	−300 ± 500	<200	300 ± 500
trans-[Ru(4-C═$CHC_6H_4NO_2$)Cl(dppe)$_2$]PF_6 (**30**)	476 (1.7)	1130	180	250 ± 300	<50	250± 300
trans-[Ru(4-C≡$CC_6H_4NO_2$)Cl(dppe)$_2$] (**31**)	477 (2.0)	351	55	320 ± 55	<50	320 ± 55
trans-[Ru{(*E*)-4,4′-C═CHC_6H_4CH═$CHC_6H_4NO_2$}Cl(dppe)$_2$]PF_6 (**32**)	473 (1.5)	441	74	650 ± 500	<50	650 ± 500
trans-[Ru{(*E*)-4,4′-C≡CC_6H_4CH═$CHC_6H_4NO_2$}Cl(dppe)$_2$] (**33**)	489 (2.6)	2676	342	40 ± 200	<100	40 ± 200

[a] Conditions: measurements were carried out in thf; all complexes are optically transparent at 800 (γ) and 1064 (β) nm. β values are ±10% and corrected for resonance enhancement at 532 nm using the two-level model with $\beta_o = \beta[1 - (2\lambda_{max}/1064)^2][1 - (\lambda_{max}/1064)^2]$; damping factors not included. γ values are referenced to the hyperpolarizability of thf (1.6×10^{-36} esu). [b] Not determined (solution showed excessive light scattering). [c] CH_2Cl_2 solvent. [d] Reference 7. [e] Reference 41. [f] Reference 31. [g] Reference 6. [h] Tail to lower energy extends to >400 nm in the visible region. [i] Not determined.

larizability.[49] The low-energy band for these complexes is the MLCT band; as the higher-energy bands for chlorobis(bidentate phosphine)ruthenium alkynyl complexes are associated with transitions involving other ligands,[41] with little change in dipole moment between ground and excited states (and hence only a small contribution to the optical nonlinearity), it is possible that the two-level corrected values may have some significance as an indicator of frequency-independent nonlinearity.

Inspection of the data for the precursor acetylenes reveals that β and β_0 increase upon increasing acceptor strength (proceeding from **7** to **2**), chain lengthening (proceeding from **2** to **3** and then **4**), and introduction of an ene linkage (proceeding from **3** to **4**), which are well-established structure−NLO activity trends for organic donor−bridge−acceptor molecules. Examination of the data for the vinylidene and alkynyl complexes reveals the following trends.

(i) Proceeding from organic acetylene to organometallic vinylidene or alkynyl complex by incorporation of the electron-rich ligated metal (functioning as a strong donor group) results in a significant increase in β and β_0.

(ii) Introduction of an acceptor group and increasing acceptor strength (proceeding from aryl 4-H to 4-CHO to 4-NO_2) results in progressively increasing β and β_0.

(iii) Chain lengthening in proceeding from **19** and **21** to **23** results in increased β and β_0. Surprisingly, proceeding from **19** to **21** does not result in a significant increase in β_{exp} or β_0. It has been shown with organic compounds that "chain-lengthening" arylalkynes leads to a saturation of the β response for two repeat units, whereas the β response for oligo(phenylenevinylene) compounds does not saturate until the complex contains approximately 20 repeat units.[50] The present compounds afford an unusual series for which minimal increase in β_{exp} or β_0 (within the error margin of ±10%) is seen on progressing from $n = 0$ to 1 for *trans*-[Ru{4-C≡C(C_6H_4-4-C≡C)$_n$$C_6H_4NO_2$}Cl(dppm)$_2$], but a significant increase is seen on progressing to $n = 2$. For this series of complexes, increasing β is not correlated with a red shift in λ_{max}; chain lengthening is accompanied by a blue shift in optical absorption maxima.

(iv) Replacing an yne linkage by an ene linkage results in increased β and β_0.

(*v*) The effect of wholesale ligand replacement (replacing Cl(pp)$_2$ with $(PPh_3)_2(\eta$-$C_5H_5)$) or coligand modification (replacing dppm with dppe) is not clear-cut. The lack of a consistent effect on β of coligand variation correlates with the lack of impact on oxidation potential and a very minor red shift in optical absorption maxima on replacing dppm with dppe for these complexes. Although $Ru^{II/III}$ couples are largely invariant on proceeding from the cyclopentadienyl bis(triphenylphosphine) complex to the chloro bis-dppm complex analogue, there is a significant red shift (13−18 nm) in optical absorption maximum; for the present series of

complexes, though, this does not correspond to a consistent increase in β_{exp}.

The present series of data also provide the opportunity to assess the effect of deprotonation, in proceeding from the vinylidene complex to the alkynyl derivative. One would perhaps expect that replacing the electron-rich ruthenium donor in the alkynyl complexes with a cationic ruthenium in the vinylidene complexes would result in a significant decrease in nonlinearity, but this is not observed; some vinylidene/alkynyl complex pairs have similar nonlinearities (e.g., **16** and **17**; **18** and **19**; **24** and **25**), and in some instances β(vinylidene) > β(alkynyl complex) (e.g., **28** and **29**; **30** and **31**). The reason for this unexpected result is not known. Other vinylidene/alkynyl complex pairs follow the "expected" trend with β values. The β_{exp} and β_0 values for vinylidene/alkynyl complex pairs differ by factors of >3 (**30** and **31**) and > 6 (**32** and **33**), differences sufficient to readily distinguish β signals into bi-stable "off" and "on" states. As the alkynyl complexes can be reprotonated to afford the precursor vinylidene complex, and this sequence can be repeated, these complex pairs can provide a protically switchable NLO-active system where the "on" signal can be either the vinylidene (**30**) or alkynyl complex (**33**).

Cubic Hyperpolarizabilities. Third-order nonlinearities of complexes **12**−**21** and **23**−**33**, together with those of some of the precursor acetylenes, were determined by Z-scan measurements at 800 nm. Results for the precursor acetylenes are consistent with their having modest $|\gamma|$ values consisting of a positive real component (γ_{real}) and a small (in some cases, not detectable) imaginary (γ_{imag}) components, and with an increase in cubic nonlinearity on chain lengthening. Nonlinearities of the vinylidene and alkynyl complexes are characterized by large error margins in many instances, rendering extraction of structure−property relationships difficult, and negative real components and significant imaginary components for many of the complexes, indicative of two-photon resonance effects. Nevertheless, two points may be noted.

(i) As observed with β_{exp} and β_0 trends, the effect of chain lengthening on $|\gamma|$ is insignificant within error margins on proceeding from **19** to **21**, but there is a dramatic increase in $|\gamma|$ in proceeding to **23**.

(ii) Vinylidene/alkynyl complex pairs **16**, **17** and **18**, **19** have significantly greater γ_{imag} values for the alkynyl complexes **17** and **19** than for their related vinylidene complexes **16** and **18**. γ_{imag} is related to the two-photon absorption (TPA) cross-section σ_2. TPA has attracted considerable recent interest for possible applications such as multiphoton microscopy and data storage.[51] The order of magnitude variation on γ_{imag} values for vinylidene/alkynyl complex pairs in this system provides protically switchable materials in which the TPA response can be alternatively switched "on" (**17** and **19**) and "off" (**16** and **18**).

Acknowledgment. We thank the Australian Research Council (M.G.H.), the Fund for Scientific Research-Flanders (G.0338.98, G.0407.98) (A.P.), the Belgian Government (IUAP−IV/11) (A.P.), and the KU Leuven (GOA/2000/03) (A.P.) for support of this work, and Johnson-Matthey Technology Centre (M.G.H.) for the generous loan of ruthenium salts. N.T.L. was the recipient of an Australian Postgraduate Award, and M.G.H. holds an ARC Australian Senior Research Fellowship.

Supporting Information Available: Tables of crystal data, positional and thermal parameters, and selected bond lengths and angles. This material is available free of charge via the Internet at http://pubs.acs.org.

OM0101700